

# Comparative Analysis of Thermal LiDAR and Multispectral Data Models for Remote Sensing in Siegerswoude, Netherlands.



Figure 1: photo operating drone during fieldwork (own work)



UNIVERSITY OF AMSTERDAM



**4D Research Lab**

Student name:	Kevin Wilhelmus Johannes Hovens
Student number:	479959
University:	Hogeschool Saxion, Deventer
Faculty:	BBT Archeologie
Originator:	4D Research Lab – University of Amsterdam
Contact person:	Dr. Jitte Waagen
Thesis supervisor:	Roeland Emaus
Data:	26-01-2001
Version:	2.0

## Preface

With great pleasure, I write this preface for my graduation project on archaeological prospection and remote sensing, specifically employing multispectral, LiDAR, and thermal sensors. Through this research, my aim was to gain a comprehensive understanding of how to effectively use multispectral data and remote sensing technologies. This endeavour provided me with the opportunity to acquire new skills, familiarize myself with the latest methodologies, and apply this knowledge to tackle real-world challenges in these fields. It was a valuable learning experience that contributed to my professional growth and competence in this specialized area of study. This research would not have been possible without the invaluable support, guidance, and cooperation of several individuals and organizations. First and foremost, I would like to express my sincere gratitude to Dr. Jitte Waagen from the University of Amsterdam (UvA) for assigning this captivating research project. His vision and expertise played a crucial role in the realization of this project. I also extend my heartfelt appreciation to Mr. Roeland Emaus, my supervisor from Saxion University of Applied Sciences. His guidance and insights significantly contributed to the development and completion of this research. Furthermore, I would like to convey my gratitude to Mr. and Mrs. Neef, the landowners of the research area. Their hospitality, willingness to share information, and provision of access to the research site made this investigation possible.

*While writing this thesis, DeepL and Google translate was used for writing the text in English (UK).*

## Table of Contents

Preface.....	2
Summary.....	5
Project datasheet .....	7
1. Introduction.....	8
1.2 Outline .....	10
2. Method and Justification.....	11
3. Research & results .....	14
3.1 Research site Siegerswoude .....	14
3.1.1 Historical description.....	14
3.1.2 Soil composition .....	15
3.1.3 Groundwater level.....	17
3.1.4 Vegetation .....	18
3.1.5 Agriculture .....	18
3.1.6 Conducted research in 2019.....	18
3.2 Remote sensing techniques.....	22
3.2.1 electromagnetic spectrum.....	22
3.2.2 Multispectral.....	22
3.2.3 Optical sensors .....	23
3.2.4 Thermal Imaging.....	23
3.2.5 LiDAR.....	24
3.3 expected findings based on Section 3.1 & 3.2.....	25
3.4 Data acquisition and processing.....	25
3.4.1 Used equipment and settings.....	25
3.4.2 Data acquisition .....	26
3.4.3 Data processing .....	26
3.5 Results and comparison.....	28
3.5.1 Research results 2023, multispectral analysis.....	28
3.5.2 Research results 2023, LiDAR analysis.....	30
3.5.3 Research results 2023, optical image .....	32
3.5.4 Comparison between the 2019 and 2023 research .....	33
4. Conclusion .....	35
5. Discussion/Reflection .....	37
6. Recommendations.....	39
Bibliography.....	40

glossary.....	45
Appendix 1: data capture parameters.....	47
Multispectral survey.....	47
LiDAR survey.....	48
Appendix 2: data processing parameters.....	51
Multispectral survey.....	51
LiDAR survey.....	53
Appendix 3: coring samples.....	55

## Summary

This research involved revisiting an archaeological site in Siegerswoude, Friesland, the Netherlands, with a specific focus on remote sensing techniques. Remote sensing technology holds significant promise in archaeological research, providing a non-destructive method for archaeologists. Developed over a century, this versatile tool enables data collection from a distance, proving invaluable in monitoring crop conditions, studying landscapes, and uncovering potential archaeological sites. Various remote sensing techniques, including multispectral, thermal-infrared, LiDAR, and optical sensors, were employed. These techniques enable the detection of earthworks, subtle variations in vegetation growth, and appearances imperceptible to the naked eye. Remote sensing significantly contributes to the detection and mapping of archaeological remains, making it a valuable asset in the field of archaeology.

On the Dutch elevation map (Algemeen Hoogtebestand Nederland), researchers identified a potential archaeological site in Siegerswoude, Friesland, The Netherlands. It is linked to potential habitation associated with the outwork of Siegerswoude from the late Middle Ages, believed to be connected to agriculture and presumed to have ceased in the 18th century. This led to a thermal infrared study by the University of Amsterdam in 2019, resulting in an archaeological excavation in the same year by The Cultural Heritage Agency of The Netherlands.

The geology in the research area, starting from 0.5 meters below the surface, includes the "Laagpakket van Gieten," indicating a clay/loam area deposited during the Saale Glaciation era. Above this, the soil is attributed to the "Formatie van Bostel"; "laagpakket van Wierden," suggesting periglacial aeolian deposition with drift sand characteristics. Based on archaeological excavations, the soil structure includes an A-horizon with characteristics of a B/E-horizon, where a modest quantity of artificially introduced loam is present. The natural substrate (C-horizon) comprises light brown sand with a minimal amount of gravel, with loam becoming frequent at a depth of 60 centimeters.

During drone flights on September 21, 2023, unfavorable weather conditions limited the use of thermal-infrared and optical sensors, but multispectral sensors and LiDAR were employed. The multispectral data acquisition used a DJI M300 drone with a Micasense RedEdge sensor, providing insights into crop marks. The LiDAR survey, conducted with a DJI M300 drone featuring a Zenmuse L1 sensor, revealed earthworks and terrain morphology.

During the analysis of the multispectral data model, a rectangular plot boundary, a filled-in ditch, and an L-shaped arrangement of dots were observed. Tractor tracks and fertilization lines introduced noise to the data models, making archaeological traces and crop marks less distinguishable. In the LiDAR analysis, a rectangular plot boundary, disturbances from the 2019 excavations, a filled-in ditch, scattered lines representing additional plot boundaries, and an L-shaped arrangement of dots were observed. Agricultural influences such as manure injection lines and tractor tracks were visible. The optical image analysis revealed features corresponding to those identified in multispectral and LiDAR images. However, the L-shaped arrangement was identified as molehills.

Comparing data from 2019 to 2023, the 2023 research covered a considerably larger area, showing improvements in visibility. Noteworthy differences included the visibility of remnants from the 2019 excavation and variations in the visibility of plot boundaries on multispectral,

LiDAR, and optical images. The noise from agricultural activities was less intrusive in thermal remote sensing data models compared to multispectral and LiDAR data models, as thermal data is less affected by vegetation-related changes induced by agricultural practices.

The research revealed that multispectral sensors can effectively capture subtle variations in vegetation stress, identifying archaeological features in Siegerswoude. This underscores the substantial impact of vegetation stress on the detection of archaeological traces through multispectral remote sensing. Despite being conducted under less-than-ideal weather conditions, the observations highlight the significant potential of multispectral analysis for archaeological prospection. It's noteworthy that, in this case, superior results were achieved using LiDAR sensors.

The assessment of this research emphasizes the impact of adverse weather conditions on drone flights, potentially influencing the quality of the collected data. Limited flying opportunities due to individual schedules also hindered a thorough understanding of how multispectral data would appear under different conditions with varying vegetation stress, making it difficult to draw definitive conclusions. As a result, it is recommended to revisit Siegerswoude at various times and in diverse weather conditions. This approach will generate multiple multispectral data models from different periods and weather conditions in the same research area, facilitating a more comprehensive and reliable conclusion regarding the main research question.

## Project datasheet

<b>Name project</b>	A comparison between thermal, LiDAR and multispectral data models in Siegerswoude, Netherlands.
<b>Date (from – to)</b>	09/2023 – 12/2023
<b>Author of report</b>	Kevin Hovens, Student Saxion Hogescholen
<b>Project initiators</b>	<b>Kevin Hovens, Jitte Waagen</b>
<b>Execution</b>	Kevin Hovens, fieldwork, research, data modelling, Reporting.
<b>Scientific advice</b>	NA
<b>Delivered product(s)</b>	Projected sensor data, raster files, generated maps/visualisations, and report
<b>Where to access main outcomes/product</b>	Available on request at the 4D Research Lab. Contact Jitte Waagen (j.waagen@uva.nl)
<b>Location and accessibility of project files</b>	4D Research Lab archive, cloud storage. Available on request at the 4D Research Lab. Contact Jitte Waagen (j.waagen@uva.nl)
<b>Related publications</b>	<p>Waagen, J., Sánchez, J. G., van der Heiden, M., Kuiters, A., &amp; Lulof, P. (2022). In the Heat of the Night: Comparative Assessment of Drone Thermography at the Archaeological Sites of Acquarossa, Italy, and Siegerswoude, The Netherlands. <i>Drones</i>, 6(7), 1-21. <a href="https://doi.org/10.3390/drones6070165">https://doi.org/10.3390/drones6070165</a></p> <p>Doesburg, J. van, Heiden, M. van der, Waagen, J., Os, B. J. H. van, &amp; Meer, W. van der. (2022). Op zoek naar lijnen: De waarde van elektromagnetische inductie en optische en thermische infraroodbeelden in Siegerswoude (Friesland). Rijksdienst voor het Cultureel Erfgoed.</p>

## 1. Introduction

This research was conducted as part of a graduation project for the Archaeology program at Saxion University of Applied Sciences. The research was carried out in the first semester of the 2023-2024 academic year. The project was commissioned by the 4D Research Lab at the University of Amsterdam (UvA) and supervised by Dr. J. Waagen from UvA. Additionally, Mr. R. Emaus from Saxion University of Applied Sciences provided supervision for the project. The project aimed to explore the potential of drone remote sensing techniques, utilizing a multispectral camera and LiDAR sensors, to identify potential crop marks and earthworks.

Remote sensing provides a non-destructive approach to conducting archaeological research without disturbing the soil. The term "remote sensing," which implies observing from a distance, involves the utilization of specialized equipment to collect data that can be analysed for various purposes (Rensink et al., 2022, p. 4), including monitoring crop damage by means of drones and satellites. It is particularly valuable in archaeology for studying landscapes and uncovering potential archaeological sites. This can help archaeologists identify and monitor threats to the site, and provide a comprehensive overview of spatial features while relating them to the environment. Additionally, it can contribute to making predictions based on this information (Comer, 2014, p. 29). The development of remote sensing has been ongoing for over half a century (Scollar et al., 2009, p. 1). The earliest applications of remote sensing in archaeology date back to the 1920s. Aerial photography was used to detect archaeological features, with the technique primarily evolving in Europe until the 1970s. After that period, especially in the twenty-first century, there has been a shift in the techniques used and ongoing experiments continue to explore approaches of remote sensing in archaeology. This shift involves the use of different sensors that acquire data across the so called electromagnetic spectrum (Orlando & Villa, 2011, p. 147). The electromagnetic spectrum encompasses the entire range of electromagnetic waves, both visible and non-visible wavelengths. Sensors used in this research will capture wavelengths from this spectrum, playing a crucial role in remote sensing for gathering diverse information about archaeological sites (Waagen, 2022, p. 1). Because the application of remote sensing largely originates from outside the field of archaeology, awareness and knowledge about it are fragmented and not equally well-known among all stakeholders in the archaeological field. Therefore on the initiative of the Cultural Heritage Agency of The Netherlands, a report was released in 2022 (Rensink et al., 2022). On top of that remote sensing isn't integrated in the Dutch quality handbook for archaeology (Kwaliteitsnorm Nederlandse Archeologie). Hence, the research has been written in such a way that not only specialists with a background in remote sensing but especially the average archaeologist can follow this study.

In 2019, the University of Amsterdam conducted a thermal infrared study in Siegerswoude, Friesland, The Netherlands, to investigate possible habitation from the late Middle Ages linked to the outwork of Siegerswoude. This habitation is presumed to be associated with agriculture, with a presumed end date in the 18th century (Doesburg et al., 2022, p. 86). The initial thermal infrared study provided fresh insights into the archaeology of the area. The research suggests a potential link between observed archaeological traces and divergent vegetation (Waagen et al., 2022, p. 9), as the vegetation above these traces might exhibit distinct growth patterns compared to the surrounding areas. Multispectral cameras prove valuable in observing these differences. These distinctions become clearer during a period of vegetation stress, which occurs when unfavourable conditions hinder the normal physiological processes and growth of plants.

Stress may occur due to factors such as diseases, extreme temperatures, a period of drought, or other environmental challenges (Verhoeven, 2012, p. 133-134). This raised interest in the impact of vegetation stress on the detection of archaeological traces through multispectral remote sensing and sets the stage for a comparative analysis. This analysis compares a thermal infrared and photogrammetry study from 2019 in the same research area with new data collected in the current project. The approach of employing not only similar but also alternative remote sensing techniques makes the site compelling for revisiting. Hence, the objective of the research was to gather multispectral remote sensing- and LiDAR data, process the data, and thereby see how these contribute to a better understanding of the archaeological site, and how

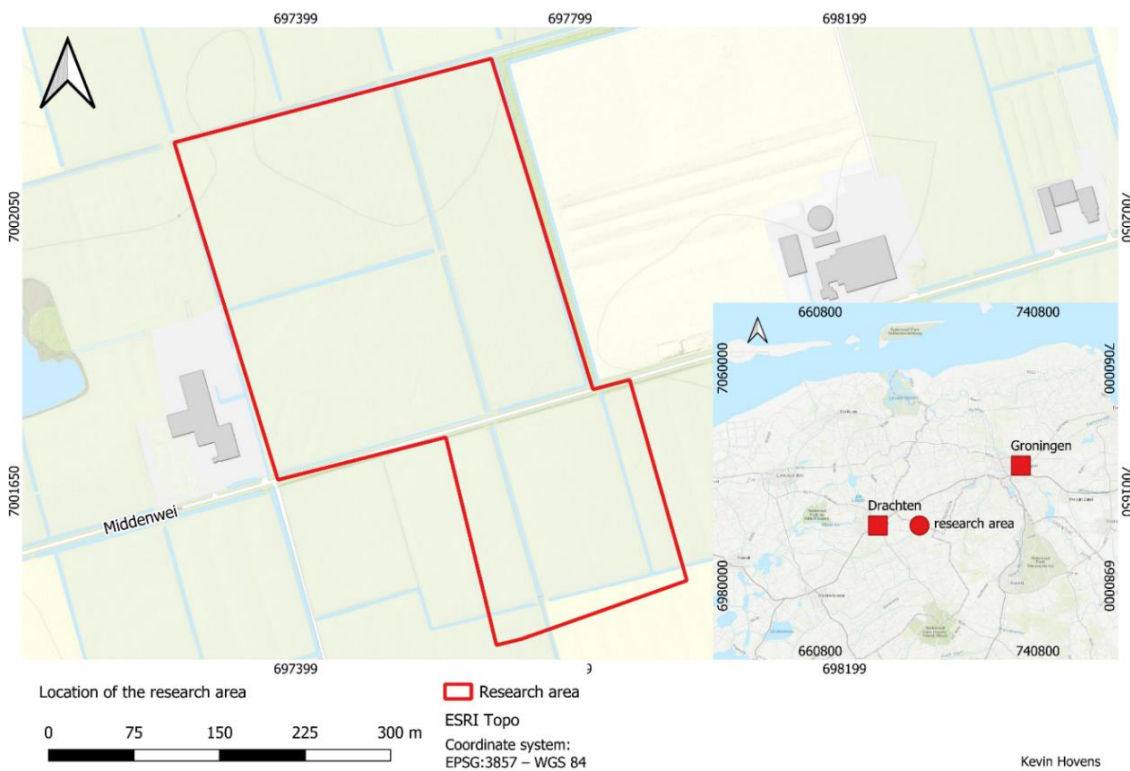


Figure 2: research area

they may contribute to new applications/methods of archaeological prospection.

To effectively manage the research question within a tight 20-week timeframe, a main research question was formulated, along with associated sub-questions. The subject of remote sensing, and in this case, multispectral remote sensing, is a very broad topic, allowing for numerous avenues of exploration. Hence, the decision was made to initiate a follow-up to the 2019 research, with a particular focus on the impact of vegetation stress. The main research question is as follows:

What is the impact of vegetation stress on the detection of archaeological traces through multispectral remote sensing in Siegerswoude?

To address the main research question, seven sub-questions have been formulated at both the micro and meso levels. Sub-questions one and two, at the meso level, delve into the methodology and techniques behind remote sensing. The remaining five sub-questions, at the micro level, focus on specific information within the study area. The sub-questions are as followed:

Meso research level:

1. What is multispectral remote sensing?
2. How can crop marks be recognized using multispectral data?

Micro research level:

3. What types of vegetation are present at the research site in Siegerswoude?
4. What is the soil composition at the research site in Siegerswoude?
5. What are the expected findings that may be observed during the analysis of the new data models based on the research activities from 2019 in Siegerswoude?
6. What are the requirements for obtaining high-quality data during the multispectral remote sensing research in Siegerswoude?
7. How does the expectation based on the 2019 research in Siegerswoude differ from the observations obtained from the multispectral data?

## 1.2 Outline

In this research, we investigate the impact of vegetation stress on multispectral data in archaeology. To address this, Section 2 outlines the research methodology. In section 3.1, details about the research area are presented, highlighting key elements such as historical context, soil composition, groundwater levels, vegetation, and agricultural activities. Subsequently, the section provides the findings of the research conducted in 2019. Subsequently in Section 3.2, it elucidates the remote sensing techniques employed in this research and how they recognize crop marks or earthworks. Section 3.3 begins with what the expected finds are based on in Sections 3.1 and 3.2. Section 3.4 details the fieldwork procedures and data processing methods. In Section 3.5, the 2023 results for each remote sensing technique are presented, followed by comparisons with the 2019 results. Finally, Section 4 encapsulates the conclusion, discussion, and recommendations.

## 2. Method and Justification

During the research, a decision was made not to answer the sub-questions in sequential order. Therefore, in the results chapter, sub-question 1 & 2 were interchanged with 3 & 4. The reason for this decision was that it seemed more logical to first investigate specific information about the research area, including the historical context, geology, geomorphology, soil composition, vegetation, agricultural activities, and the findings from the 2019 study (Section 3.1). Subsequently, research was conducted using various sensors. Throughout this study, multispectral sensors, LiDAR, and aerial photographs were employed, along with the thermal sensor data from 2019. In addition to detailing the techniques used, this section also describes the recognition of crop marks or earthworks (Section 3.2). This provides a general understanding of how the sensors work and how they can be used to observe archaeological features. By answering sub-questions 1 to 4, a foundational knowledge is established to describe the expected findings that may be observed during the analysis of the new data models. Hence, this is addressed in Section 3.3. With this knowledge in mind, drone flights were conducted on September 21, 2023. The materials used, the description of the field day, and the data processing are therefore described in Section 3.4. Following data processing, the analysis begins, conducted separately for each sensor: Multispectral, LiDAR, and then optical sensors. Subsequently, a comparison is made, aligning the expected findings based on information from 2019 research with that of 2023. An attempt is made to explain the differences and the reasons behind them.

Method per research question:

### 1. *What is multispectral remote sensing?*

To address sub-question one, the chosen research methodology involves conducting a literature review, wherein a minimum of Waagen et al. (2023) and Verhoeven (2012) must be utilized. This approach is considered the most suitable due to the extensive existing literature on multispectral remote sensing and the associated methodologies and limitations. However, the sheer volume of available literature poses challenges in discerning crucial information. Furthermore, it is worth noting that while there is a considerable body of literature on these topics, most of it is related to other fields besides archaeology, with an emphasis on agriculture.

### 2. *How can crop marks be recognized using multispectral data?*

To address sub-question two, a literature review will be conducted, with Verhoeven (2012) and Cartreul (2017) as the primary sources. This approach is considered the most suitable due to the existing literature about how crop marks occur and how they can be recognized using multispectral data. Similar to sub-question one, most literature on this topic is related to other fields besides archaeology.

### 3. *What types of vegetation are present at the research site in Siegerswoude?*

In addressing sub-question three, the research approach incorporates a combination of information from the landowner, a literature review, and inventory fieldwork. The landowner can provide information about the vegetation that has been planted in the past years. Furthermore Wageningen University & Research has published a handbook for livestock farming (Remmelink et al., 2020). In this handbook, various plant types and their characteristics are described. Additionally, the handbook includes a form on how to recognize certain plant types. This form is utilized during the fieldwork to determine the specific plant species in the research area, with a focus on grass types. These methods are well-suited for this purpose as they

provide insights into the current environmental conditions and offer historical context. One limitation could be that during the fieldwork, no specific plant types could be identified.

*4. What is the soil composition at the research site in Siegerswoude?*

Sub-question four will be addressed primarily through a literature review, data analysis, and map analyses. This approach is considered sufficient due to the availability of numerous sources. Specifically, the Dinoloket database (TNO Geologische Dienst Nederland, 2023), containing soil drillings with information about the soil in the research area, will be utilized. Additionally, two maps will be used: the soil map (Kadaster, 2022) and geomorphology map (Kadaster, 2003). Although the possibility of conducting a soil survey was considered, it was ultimately not pursued due to regulatory constraints and the information already available. Similar data is already present in an excavation report from this exact research location (Doesburg et al., 2022). The limitation of this method is that the existing information about the soil in the research area mostly represents a small portion of the total area, except for the two maps. Nevertheless, it is reasonable to assume that the soil characteristics are relatively consistent throughout the entire area.

*5. What are the expected findings that may be observed during the analysis of the new data models based on the research activities from 2019 in Siegerswoude?*

Sub-question five will be addressed through a literature review. Three papers describe previous research activities and their results in this area (Doesburg et al., 2022; Rensink et al., 2022; Waagen et al., 2022), making this method the most suitable. The results from those three studies, the knowledge about multispectral sensors (sub-questions 1, 2), and the information about the research area (sub-questions 3 and 4) are used to formulate the expected findings. These findings are the anticipated results during the analysis of the new data models.

*6. What are the requirements for obtaining high-quality data during the multispectral remote sensing research in Siegerswoude?*

For research sub-question six, a combination of a literature review and information from J. Waagen will be utilized. These methods are considered the most appropriate because existing information on how to operate and prepare for the research already exists. The expert's guidance is invaluable, particularly for aspects of the process that may not be extensively documented but rely on practical knowledge, such as specific drone operation settings. It's important to note that by "high-quality data," it is referred to as data of such calibre that is suitable for conversion into .TIFF format and enables visual analysis. While we did contemplate interviews, they weren't deemed feasible as the expert can offer real-time information throughout the research. The potential risk of overlooking information is mitigated by the expert's experience, and the use of a mandatory flight format helps ensure comprehensive coverage. Because the equipment and methods used in this study are provided by the commissioner, the University of Amsterdam, alternatives are not considered. Additionally, other reports from the University of Amsterdam indicate that the methods can yield results (Waagen, 2023).

**7.** *How does the expected findings based on the 2019 research in Siegerswoude differ from the observations obtained from the multispectral data?*

Sub-question seven will involve the post-processing of results using multiple research methods: data analysis and data comparison. These methods are suitable for addressing the question as they involve the analysis of new data collected in 2023, followed by a narrative comparison with data and findings from 2019. By presenting it in a narrative manner, the research becomes more accessible for the average archaeologist without a background in quantitative methods. The primary limitation is the potential for problems during fieldwork or data corruption, which could impede the analysis. Therefore, no alternative research methods are being considered, as data analysis and comparison are deemed straightforward and effective for obtaining the necessary information.

### 3. Research & results:

#### 3.1 Research site Siegerswoude

In this Section, specific information about the research area is provided. Firstly, a brief overview of its history, followed by details on soil composition, groundwater levels, and vegetation. Afterward, previously conducted archaeological and thermal infrared research from 2019 and its results are discussed.

##### 3.1.1 Historical description

According to historical records, the village of Siegerswoude is first mentioned in the fourteenth century AD (Worst & Zomer, 2011, p. 33). In the area, there was a former monastery of the Benedictines at village Smalle Ee. This monastery had a subsidiary outwork in Siegerswoude mainly inhabited by women, first mentioned in historical sources in 1518. The people living in the outwork were involved in several boundary disputes and kept sheep in the surrounding areas (Worst, 2012, p. 84). The estate also featured an area of cultivated land. The revenue from the outwork would have primarily supported the Smalle Ee monastery. In 1581, on the orders of the States of Friesland, the outwork was set was destroyed to prevent the Spanish army from taking advantage (Doesburg et al., 2022, p. 24). Historical maps from the eighteenth century AD show a marking with six dots at the site (figure 3). The dots could be interpreted as old houses.

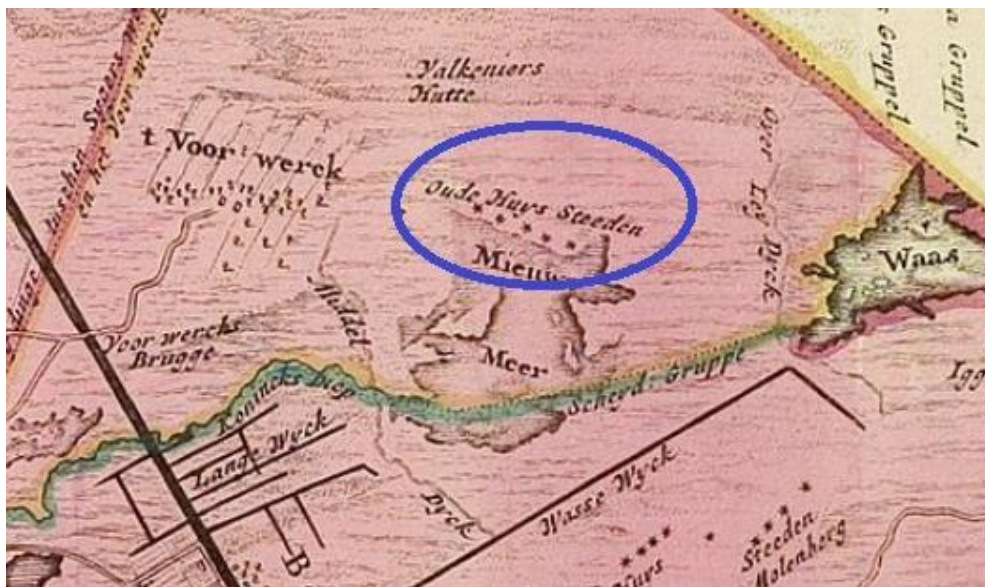


Figure 3: map from Schotanus, 1698, scale 1: 37000 (Schotanus, 1718) .

On the Dutch LiDAR dataset (Algemeen Hoogtebestand Nederland), at the location, five to nine large square plots can be observed (Figure 4). This suggests the possibility that the rectangular plots may have belonged to a house, with agriculture conducted on the surrounding plots (Waagen et al. 2022: 8-12). On the initiative of the Noord-Nederlandse Cultuurvereniging, a systematic reclamation project took place in Siegerswoude from 1910 to 1916. In that project, eleven farms were also constructed, including that of the Neef family, the owners of the research area. (Doesburg et al., 2022, p. 29).

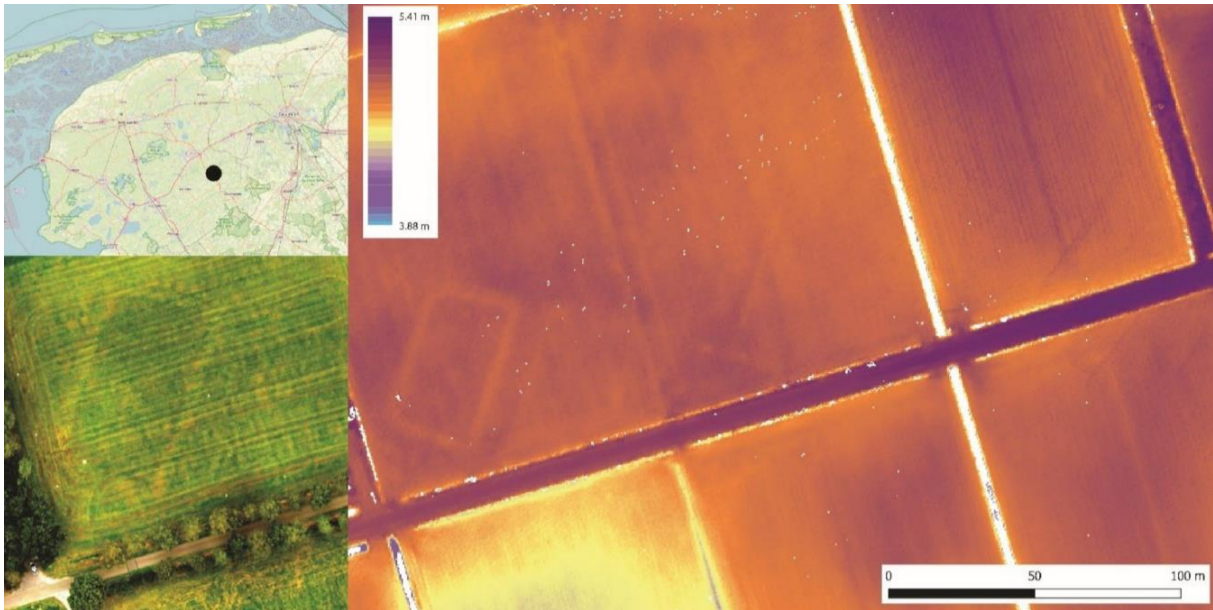


Figure 4: map featuring AHN data, drone orthophoto, location, and rectangular plots (Waagen et al., 2022, p. 8) .

### 3.1.2 Soil composition

This section provides a description of the soil composition and formation. A challenge lies in the use of specific Dutch names because they are difficult to translate. Therefore, the Dutch terms will be used and explained in this section. On the database of Dinoloket.nl, information is available about six soil corings close to the research area (figure 5). In Appendix 3, the detailed coring samples are provided. Five out of the six samples have a similar description, except for one. Generally, from top to bottom, the uppermost layer consists of sand fine-grain category, followed by a sand medium-grain category, and then a loam layer. In corings B11F0946, B11F0838, and B11F0837, in the middle of the loam layer, a sand medium-grain category can be found one coring, B11F0837, is different, as it features a peat layer situated between the sand

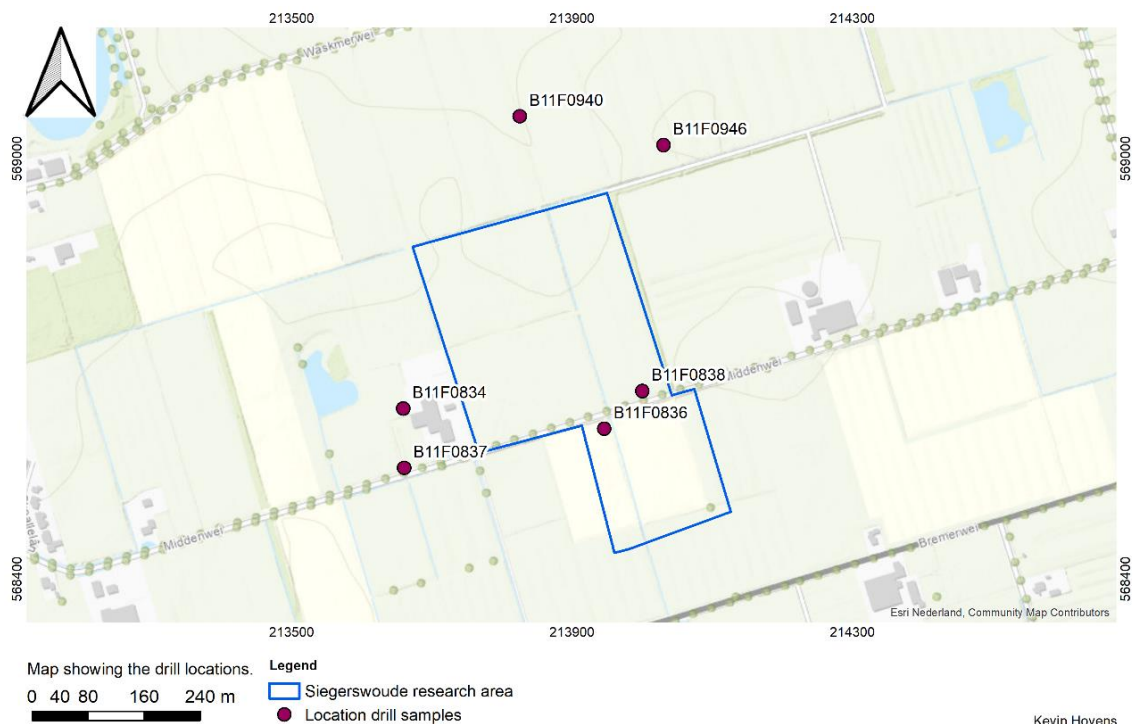


Figure 5: research area with the coring locations (TNO Geologische Dienst Nederland, 2023; own work)

Kevin Hovens

fine-grain and sand medium-grain categories. Based on the information obtained from the corings the geology in the area, starting from 0.5 meters below the surface, is composed of the "Laagpakket van Gieten." This means that the region is situated in a clay/loam area deposited during the Saale Glaciation era (TNO Geologische Dienst Nederland, 2023a). The soil above has been deposited by the "Formatie van Boxtel"; "laagpakket van Wierden." This implies the presence of periglacial aeolian deposition, characterized by drift sand (TNO Geologische Dienst Nederland, 2023c).

Looking at the geomorphology in the area (Figure 6), the research area is situated in a terrain of "grondmorenenwielving," this glacial deposition occurs when land ice transports material underneath the ice creating a undulation soil. In the northeastern section of the research area, there exists a geological feature known as the "vlakte van grondmorene," which is comparable to "grondmorenenwielving;" however, in this case, the ground is compressed into a flat plain. Moving southward from the research area, an aeolian deposition identified as the "dekzandrug" (cover sand ridge) comes into view. These elevations originate from blown sand during the Weichselian period, typically displaying an elongated form. To the south of the "dekzandrug," fluvial depositions, specifically labelled as "beekdalbodems" (brook soil) and "glooiing van beekdalzijde" are present. The term "beekdalbodem" signifies the formation of a valley resulting from the erosive action of a river or stream. This process is accompanied by the creation of fluvial terraces, forming a distinct sharp edge. The presence of "glooiing van beekdalzijde" in the same area indicates that the edges, shaped by the "beekdalbodem," exhibit a sloping terrain. In the western part of the research zone, a geological formation known as a "dalvormige laagte" is situated. This periglacial deposition shares similarities with a "beekdalbodem" but lacks any association with a river system (Maas et al., 2021). Finally, encircling the research area are three designated spots known as "laagte zonder randwal." These depressions lack rim embankments,



Figure 6: geomorphological map, The Netherlands, scale 1:50.000 (Kadaster, 2022).

forming closed layers enclosed by small sand embankments. The nature of these areas may vary, ranging from marshy to non-marshy conditions (ten Cate & Maarleveld, 1977, p.77).

The process by which the previously mentioned "grondmorenewelving" is formed results in a layer consisting of "keileem," a type of soil consisting of a of sand, clay, loam and rocks. The "keileem" in the research area (Figure 7) are covered with "veldpodzol soil, characterized by loamy and weakly loamy fine sand." This soil type has a characteristic and highly humic black topsoil (A-horizon). This indicates that these soils were previously covered with peat. Beneath this layer, there is a dark gray leaching horizon (E-horizon), followed by a leaching layer (B-horizon) (Doesburg et al., 2022, p. 15). There are five additional soil types in the surrounding area (Figure 7). The other soil types are further explained in the Glossary list.

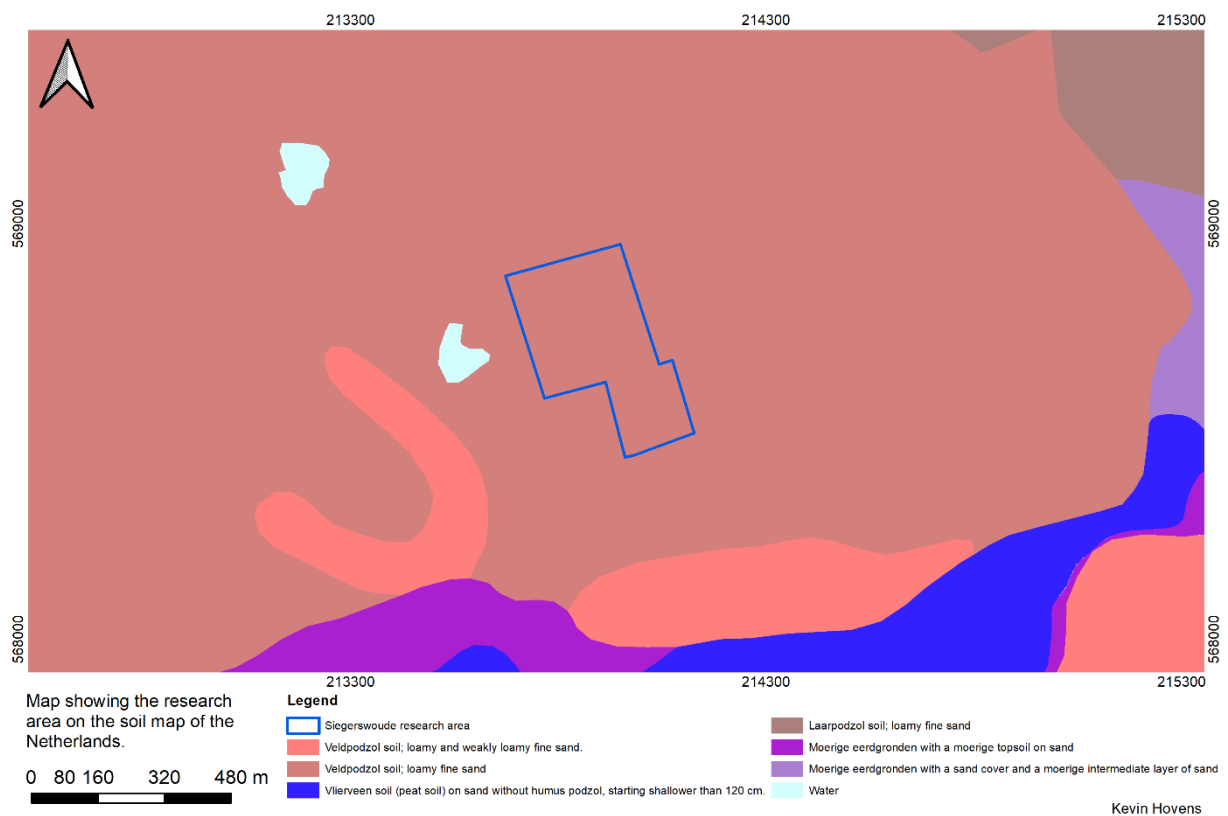


Figure 7: soil map, The Netherlands, scale 1:50.000 (Kadaster, 2003).

### 3.1.3 Groundwater level

In the research area, the groundwater level typically ranges from a minimum average depth of 45 centimetres beneath the surface to an average maximum depth of 150 centimetres beneath the surface. This data reveals an annual fluctuation of approximately one meter in the groundwater level. And an average depth of 60 centimetres beneath the surface during the spring season (TNO Geologische Dienst Nederland, 2023). In theory, it is worth noting that this fluctuation could potentially affect the archaeological remains (Willemse, 2020, p. 25). Although these effects won't be observed during this study.

### 3.1.4 Vegetation

For the research, it is essential to understand the specific sorts of vegetation present. This is because different plant species have distinct characteristics, such as the chlorophyll content (Section 3.2.2). According to Boer&Bunder.nl (2023), the entire study area is categorized as permanent grassland. However, it is important to note that there are various grass species that can be used for grassland. When establishing grassland, a mixture of different grass species is advised during seeding. The selection of the specific grass mixture and species for seeding depends on factors such as climate, fertilizer regulations, nutrients, soil conditions, and yield. For the use of permanent grassland, mixtures are commonly employed, with English ryegrass being a fundamental component. Other species like white clover and meadow fescue are added to enhance the mixture. Nowadays, species like “*Festuca arundinacea*” and “*Festuca rubra*” are also increasingly used (Hoogendijk et al., 2021, p. 73).

During fieldwork, a specific grass species couldn't be identified using the handbook from Wageningen University & Research (Remmelink et al., 2020, pp. 3.2-3.8). The landowner, G.J. Neef, mentioned that the same pasture has been in place for approximately 30 years. Over time, this has led to a mixture of grass types, making it challenging to determine the specific type of grass present due to this intermingling. It is important to note that differences between grass species are not extremely significant. While one species may be more sensitive to factors like drought, rain, frost, and diseases, resulting in some form of vegetation stress (see Section 3.2), the variation is not as pronounced as when, for example, part of the area was planted with “*Zea mays* L.”

### 3.1.5 Agriculture

The research area, designated and utilized for agricultural purposes (Cropx, 2023), is regularly subjected to a variety of periodic agricultural activities, such as ploughing, fertilizing, chiselling, seeding, and the installation of drainage systems (Lascaris & Os, 2019, p11). According to the landowner, G.J. Neef, the most frequently performed agricultural activity in this research area is the application of animal manure into the land, specifically through the use of manure injection. This technique involves injecting manure into the soil, creating small incisions in the ground. Additionally, fertilization provides the land with a nutrient boost, resulting in enhanced vegetation growth (Smit & Jager, 2023, p. 20). These agricultural practices are recognized for their substantial impact on archaeological artifacts, particularly at significant depths, with the potential for deep ploughing to cause even more considerable damage to archaeological traces beneath the surface. It is noteworthy that these operations predominantly affect the topsoil, a critical consideration given that upcoming remote sensing techniques primarily emphasize surface scanning (Lascaris et al., 2019, p.55). The excavation from 2019 (Section 3.1.6) confirms what is mentioned about the significant agricultural impact on the topsoil. The soil profile (Figure 11) unveils a substantial layer that has undergone cultivation by agriculture.

### 3.1.6 Conducted research in 2019

In 2019, the Cultural Heritage Agency of the Netherlands (Rijksdienst voor het Cultureel Erfgoed or RCE) and the University of Amsterdam (UvA) conducted a thermal-infrared and optical sensor study and excavation in Siegerswoude, situated in the Dutch province of Friesland. Research using thermal-infrared technology is still experimental but has the potential to reveal archaeological traces. Using the thermal-infrared cameras, it is possible to measure a specific wavelength within the electromagnetic spectrum. These wavelengths are associated with heat

radiation submitted from underground and surface irregularities (Waagen et al., 2022, p. 1). During the thermal-infrared research in 2019, the following results were made: In Figure 8, thermal images reveal plot boundaries at points A, C, and E, distinguished by the presence of remnants of narrow ditches. Additionally, thermal images depict drainage ditches in the northeastern part of the research area, designated as letter E in Figure 8. Notably, an intriguing observation emerges from letter F in the thermal images, where a rounded rectangle is visible.

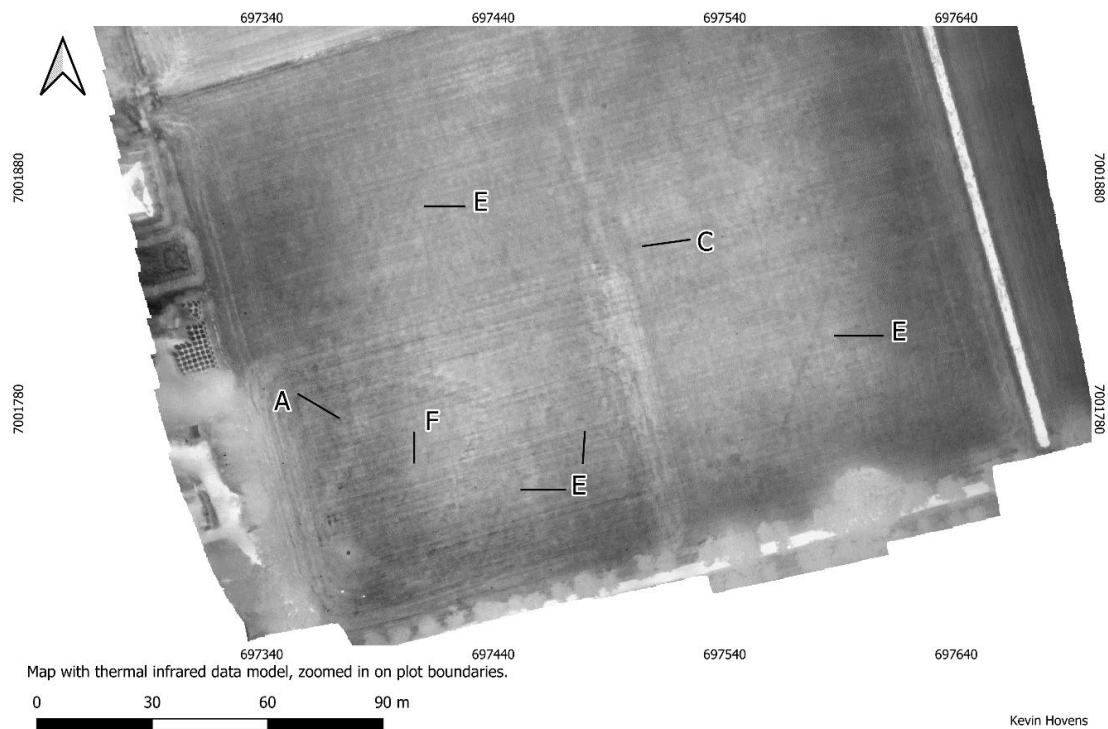


Figure 8: Thermal image Siegerswoude 2019, verkleuringen A-E (Waagen et al., 2022, p 10).

While conducting the excavation within the confined space of the narrow ditch during the excavations in 2019, it was revealed that during the 17th century, individuals had undertaken the digging of pits, subsequently inserting wooden posts into these excavated areas. The presence of such archaeological features raises the possibility that they could have constituted integral components of a historical structure or building from that era. During these excavations, a significant ditch, approximately 4 meters in width (Figure 9), was discovered in the southwest of the planning area beneath the topsoil. Its bottom was situated at a depth of about 1.5 meters relative to the ground surface. From bottom to top, the filling of this archaeological feature consists of a humic layer, followed by sods, and then a crumbly layer of clay/peat. This ditch



Figure 9: ditch, 4 meters in width (Doesburg et al., 2022, p. 55)

served the purpose of draining the peat area and extracting loam, which was subsequently utilized to elevate the surrounding terrain. In the north and east of the planning area, remnants of ditches have been found with a width of approximately 50 centimetres and a depth of 30 centimetres. (Doesburg et al., 2023, pp. 52-63; Waagen et al., 2022, pp. 9-12). A map of all features is provided in Figures 10 and 11. Furthermore, the excavations failed to identify any farmsteads. Instead, there seems to have been an effort to establish a plot boundary (Doesburg et al., 2022).



Figure 10: map of features from the excavation in 2019 on LiDAR data model (Doesburg et al., 2022, p. 53).

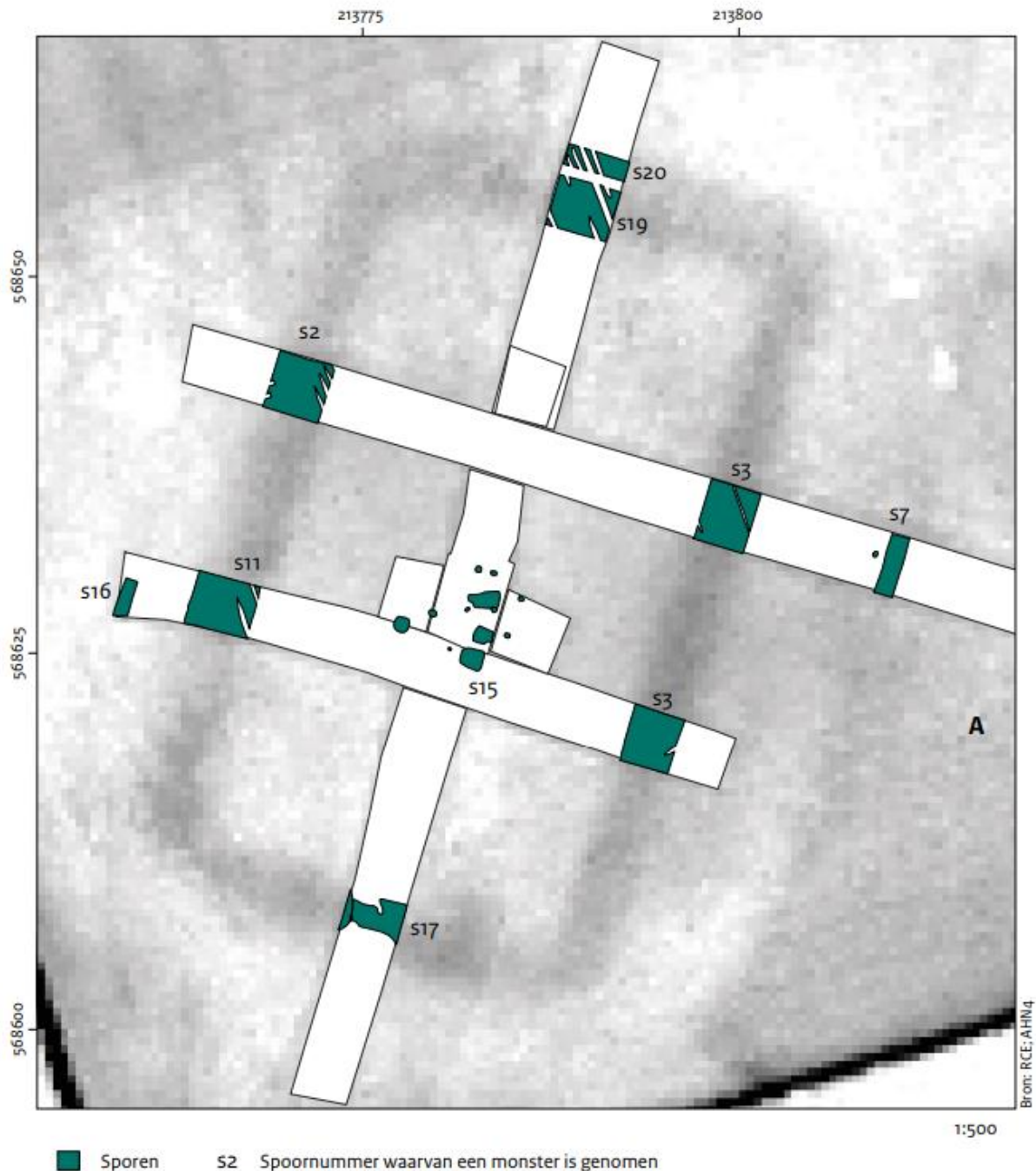


Figure 11: archaeological features map, farmstead on Thermal Infrared data model (Doesburg et al., 2022, p. 73).

Based on the archaeological excavations, the following can be said about the soil structure: The soil profile within the research area can be described as follows from top to bottom (see Figure 12): an A-horizon exhibiting characteristics of a B/E-horizon. In this layer a modest quantity of loam is present, which has experienced significant disturbance. Moreover, loam does not naturally occur in this layer, it is introduced artificially. The natural substrate (C-horizon) comprises light brown sand with minimal amount of gravel. At a depth of 60 centimetres, loam becomes frequent (Doesburg et al., 2022, p. 51).



Figure 12: example, soil profile Siegerswoude Friesland (Doesburg et al., 2022, p.51).

### 3.2 Remote sensing techniques.

In this section, the remote sensing techniques that were used will be described.

#### 3.2.1 electromagnetic spectrum

The electromagnetic (EM) spectrum comprises a wide range of electromagnetic radiation, encompassing both wave-like energy, such as sunlight, and particles, such as microwave photons. Radiation represents energy that propagates and disperses as it travels (National Aeronautics and Space Administration, 2013). Within the electromagnetic spectrum, there are discernible wavelengths: those that are visible to the human eye and those that are not. Standard aerial photographs capture wavelengths within the visible spectrum. However, multispectral sensors have the capability to detect wavelengths beyond the visible range, such as the near-infrared (NIR) wavelength, and thermal sensors can capture wavelengths in the thermal infrared spectrum. It is important to note that both visible light and the invisible spectrum consist of numerous wavelength bands, more than mentioned in this text. Different materials, vegetation, and soil can exhibit varying responses to these wavelengths, providing diverse insights into their composition. The wavelengths used in this research include blue (450-515.520 nm), green (515.520-590.600 nm), red (600-630-68-.690 nm), near-infrared (NIR) (750-900 nm) (Waagen, 2023, p. 6), and the thermal infrared spectrum (8-14 um) (Waagen, 2022, p. 1).

#### 3.2.2 Multispectral

Multispectral sensors are a technique that can measure specific wavelengths in the electromagnetic spectrum, including blue, green, red, and near-infrared. The distinct characteristics of these wavelengths enable multispectral sensors to capture valuable data about the composition and characteristics of the observed objects or surfaces (Waagen, 2023, p. 6). This capability allows for the observation of differences in surface vegetation that remain imperceptible to the naked eye. Such a feature is particularly advantageous for identifying

archaeological traces, as the vegetation above these traces theoretically exhibits distinct growth patterns compared to the surrounding areas. These differences are referred to as crop marks, influenced by various factors including soil depth, archaeological features, soil characteristics, nutrient availability, weather conditions, and crop growth (Verhoeven, 2012, p. 133-134). To optimize the interpretation of crop marks, it is possible to calculate various Vegetation Indices (VI). This involves manipulating data by relating different wavelength bands to each other. A commonly used and informative VI is the Normalized Difference Vegetation Index (NDVI). NDVI is a vegetation index that utilizes the red and near-infrared spectra in its computation. NDVI data highlights disparity between the mesophyll content of the leaf and the presence of chlorophyll pigments. These two elements are important in the process of photosynthesis and can consequently offer information about the vegetation's health (Cartreul 2017). This allows us to determine specific characteristics of the vegetation, although these characteristics represent a snapshot in time, including factors height, stress, moisture, and the crucial chlorophyll content. The light that a healthy leaf reflects appears green to us due to its chlorophyll content. If a plant is unhealthy or its chlorophyll content changes, more blue or red reflection may be mixed in. This is because the plant might experience stress. This so-called stress occurs when certain factors, such as drought period, hinder the plant's growth and reduce its chlorophyll content. Multispectral cameras, as mentioned earlier, can measure these differences. When processing the data these differences become clear. This enables the detection of potential traces or changes (Verhoeven, 2012, p. 136).

### 3.2.3 Optical sensors

Optical sensors operate within the visible spectrum of light, capturing high-resolution images. These images can be processed into orthophotos. This is a geometrically corrected aerial photograph (ESRI, 2024). Such information becomes invaluable when studying LiDAR, thermal, and multispectral data, as it facilitates a direct comparison with the orthophotos. This comparison helps in distinguishing between natural and cultural features. For instance, while analysing Vegetation Index data models, the identification of a distinct structure might pique interest. By cross-referencing this finding with the orthophotos, it might become evident that the structure in question is a modern twenty-first century fence. Therefore, the inclusion of orthophotos alongside other datasets is highly advantageous, as it provides critical context and clarification in the analysis of various geospatial data types. (Waagen, 2023, p. 5).

### 3.2.4 Thermal Imaging

Heat sensors can identify archaeological features located close to the surface that radiate heat differently. Several factors contribute to this, including volumetric heat capacity, thermal conductivity, thermal emissivity, thermal inertia, and thermal diffusivity. These factors may result in temperature disparities compared to the surrounding soil, and these distinctions can be detected using thermal sensors. Volumetric heat capacity, influenced by a feature's volume, determines its heat absorption and retention. For example, a large stone can absorb and retain more heat compared to loose sand, maintaining heat for a longer duration. Importantly, volume heat capacity determines how much heat or cold is needed to change a material's temperature by one degree Celsius (Casana et al., 2017, p. 311; Cool, 2018, p. 1 ). An important factor in thermal studies, thermal emissivity quantifies how efficiently a material reflects or emits heat radiation and is expressed as a ratio between the thermal radiation emitted from an object's surface and that from an ideal matte black surface (Casana et al., 2017, p. 311). Thermal diffusivity determines the rate at which heat travels through a material and is closely related to

heat capacity (Cool, 2018, p. 1 ). Thermal conductivity characterizes a material's ability to conduct heat. A wet soil disperses heat much better and deeper into the surroundings than, for example, dry clay, which may not distribute heat as effectively but absorbs it better. Having said that, moist soils take longer to heat up and cool down, maintaining a more constant temperature compared to dry soils. This results in wet soils reduced temperature peaks compared to dry soils. This is known as thermal inertia and is closely related to volumetric heat capacity. Understanding thermal inertia is vital for establishing optimal research conditions, especially concerning the heat flux process – how heat flows or dissipates (Casana et al., 2017, p. 311; Cool, 2018, p. 2). These factors collectively contribute to a comprehensive understanding of heat dynamics in different materials, assisting researchers in making informed choices during thermal investigations. Hence, the investigation of drone thermography remains in an experimental stage, with ongoing tests of efficient sensors and platforms, alongside an exploration of the wide range of variables that could potentially impact their effectiveness (Waagen, 2023, p. 7).

### 3.2.5 LiDAR

The emergence of light detection and ranging (LiDAR) technology has driven numerous advancements in earth and environmental sciences by facilitating precise mapping and measurement of three-dimensional properties on the occurrences on the Earth's surface (Eitel et al., 2016, p. 2). LiDAR data is acquired using lasers making a dense point cloud. This involves three methods of data collection: spatial, spectral, and temporal. Spatial data collection entails measuring the time between sending a pulse and receiving its reflection. This allows for the creation of a three-dimensional image, which is essential in producing 3D maps. Spectral information is obtained through laser return intensity (LRI), as different materials reflect light in distinctive ways. This enables the potential identification of material groups or types based on the wavelength of light. The collecting of temporal data, on the other hand, encompasses repeating the LiDAR process and storing data. This facilitates tracking changes over time, such as soil erosion, and offers insights into ongoing processes (Raj et al., 2020, pp. 1-2). During LiDAR analyses, in the case of this research project, the focus is on observing earthworks. Earthworks refer to deliberate alternations made to the natural landscape through human activities, involving processes such as excavation or reshaping of the terrain (Wallinga, 2020). For example an old filled ditch can cause a variation in surface elevation compared to the surrounding area. Essentially, the observation process entails capturing the terrain morphology. While LiDAR can physically pulse through certain vegetation, it faces limitations in pulsing through dense vegetation or a canopy. However, it can effectively penetrate the canopy by utilizing gaps in the foliage. Some of these lasers penetrate and bounce back. The returning pulses are measured, and a data model of the terrain morphology can be created. The collected data can be used to compare variations in the elevation of the soil and compare them with other data (DJI Enterprise, 2022). A good example of a LiDAR data model is the AHN version 4 (Dutch elevation map), which has a resolution of 1 point for every 20 centimetres. In contrast, a drone-mounted LiDAR system can achieve a resolution of 1 point per square centimetre, and even higher resolutions are possible (Waagen, 2023, p. 6).

### 3.3 expected findings based on Section 3.1 & 3.2

Based on Section 3.1.6, a system of plot boundaries is anticipated. These can be expected throughout the entire research area and have a minimum width of approximately 50 centimetres. These plot boundaries are situated in a grassland that has remained unploughed for 30 years. These features are closely located just beneath the topsoil. Based on 3.1.3 and 3.1.6. The water level is mostly situated beneath these features or until the middle of the feature, and therefore, it doesn't significantly affect the remote sensing results. These plot boundaries, at the top of their filling, have a layer of peat/loam beneath the topsoil (Figure 9), peat is very fertile (Zijverden & Moor, 2014, p. 77). The soil surrounding the features has a less fertile sandy composition (Figure 12). The fertility differences and soil moisture can result in uneven plant growth, potentially resulting into crop marks. Consequently, the decision was made to conduct aerial surveys using multispectral sensors (Section 3.2.2 & 3.3). Additionally, these plot boundaries may exhibit micro-morphology (Section 3.2.5 & 3.3) because the ditches from the plot boundaries are filled with material different from the surrounding area. In addition, the decision was made to also utilize LiDAR sensors during the survey. Finally, the excavations have resulted in soil disturbance, leading to a different soil composition in this area. This disturbance will be observed in the multispectral and LiDAR data models. Based on Section 3.1.5, it is anticipated that agricultural activities will be observed on the data models. These activities can potentially obscure the visibility of other traces. Finally

### 3.4 Data acquisition and processing

In this section, the used equipment and settings will be discussed. Subsequently, data acquisition details the fieldwork conditions, encountered challenges, and the execution process. Finally, in the Data Processing Section, the process of handling the collected data is explained.

#### 3.4.1 Used equipment and settings

The multispectral data acquisition was conducted using a DJI M300 drone equipped with a Micasense RedEdge sensor. The RedEdge sensor has a resolution of 1.2 megapixels, providing resolution at 1280x960 pixels. This sensor is complemented by a 5.44mm lens. The drone was flown at an altitude of eighty meters, maintaining a steady speed of 3.3 meters per second. To ensure comprehensive coverage and data accuracy, an 80/70% overlap and sideways overlap was employed. For the LiDAR survey, a DJI M300 drone was utilized, featuring a Zenmuse L1 sensor with the Livox LiDAR module. This LiDAR system achieves a point rate of 480,000 points per return. The flight was executed at an altitude of seventy meters, with a ground speed of five meters per second. The swath width extended to thirty meters, guaranteeing thorough coverage, with a 50% flight strip overlap. Additionally, the LiDAR module is equipped with a built-in optical camera, offering a resolution of twenty megapixels and an 8.8mm lens for capturing supplementary imagery (for more details, please refer to Appendix 1). During this study, the material described in this section was utilized, as it was made available by the commissioner, the University of Amsterdam. Important to note that the drone used is compatible with the sensors employed. Additionally, the Zenmuse L1, a sensor from DJI, is seamlessly integrated on a software level, enhancing overall usability. It's essential to highlight that not all sensors are compatible with the DJI M300. The initial plan included an optical drone flight with a different drone. In other words, not all drones and sensors work well together. The material used during this project is also employed by other entities. For instance, Wageningen University has a research centre that uses the same drone (Wageningen University & Research, 2023). The Micasense RedEdge is also employed by the University of Edinburgh (James et al.,

2020). Lastly the Zenmuse L1 sensor with the Livox LiDAR module has also been used by the Czech Technical University in Prague (Štroner et al., 2021).

In Section 3.3, it is mentioned that the expected traces have a minimum width of approximately 50 centimetres. The ground resolution should be such that it can capture the expected traces in at least 3 pixels, so 50cm/3, making the pixel size 17 centimetres. Now, this ground resolution is easily achievable, considering the flight was performed at a height of 70/80 meters.

#### 3.4.2 Data acquisition

On Thursday, September 21, 2023, the field research took place in Siegerswoude, Friesland, the Netherlands. During this research, there were plans to conduct flights equipped with optical, LiDAR, multispectral, and thermal infrared sensors. Unfortunately, the weather conditions were unfavourable. In the preceding week, there had been heavy rainfall, resulting in a wet ground. On the day of the research, it was raining almost constantly, and the sky remained heavily overcast throughout the day, with temperatures ranging from fifteen to twenty degrees Celsius. The grass had been recently mowed short before the flight. Despite these challenging conditions, the decision was made to proceed with flights using LiDAR and multispectral sensors. However, the planned optical and thermal flights were not carried out. The optical flight was not conducted due to weather conditions, however LiDAR data can still be utilized to create RGB data models, but with a lower resolution. The thermal flight was cancelled due to the wet ground conditions. This would have led to minimal to no temperature variations during the ideal flight times, typically in the morning or evening. Additionally, the dominant factor was the water temperature, resulting in a uniform temperature surface and making it difficult to detect significant differences (Section 3.2.4). During the flights, the drone followed a north to south trajectory in a west to east motion. During the multispectral flight, there was minimal drizzle, except in the last rows performed in the southern part of the flight plan, where heavy rain occurred, leading to the cancellation of that portion of the flight. As a result, approximately 5-10% of the intended flight route was not completed. In contrast, during the LiDAR flight, there was only a light drizzle, and the entire flight was completed successfully. However, towards the end of the LiDAR flight, a system error occurred. While this issue had been encountered before, it did not impact the data quality at that time. An interesting question arising from this situation is how rain affects LiDAR data, as discussed in Section 3.2.5. LiDAR sensors emit a significant amount of radiation, which reflects off surfaces and is recorded. Hypothetically, rain could cause premature reflections. On the other hand, the sheer volume of emitted rays often results in the majority of them still reflecting off the ground and being recorded.

#### 3.4.3 Data processing

The multispectral dataset has been processed using photogrammetric software, specifically Pix4D. For a more detailed guideline, refer to Pix4D (2023). At each moment of capture, five distinct images were generated, identified as [..]\_1.tif, [..]\_2.tif, and so on. Each of these images corresponds to a specific bandwidth and contains recorded reflectance values for the Red (R), Green (G), Blue (B), Rededge (RE), and Near-Infrared (NIR) bands. After this initial capture, the geotagged images underwent a swift manual quality inspection to ensure their suitability. Within Pix4D, a calibration process was initiated. This calibration utilized photographs taken in the field, particularly those of the reflectance target, and incorporated data in the EXIF image metadata that was gathered with the MicaSense RedEdge. This calibration step aimed to compensate for significant variations in solar radiation that may have occurred during image

acquisition. Next, the reflected data in the green band was used to perform the standard photogrammetric procedure. The green band images were used to process all other images because it contains more features of the vegetation than other bands, making it easier for Pix4D to find overlapping features and establish tie points. In Pix4D, automatic tie points were generated by analyzing different 2D images. The software identified overlaps between images and sought identical points where the lines of projection intersected. At these intersections, 3D points, known as automatic tie points, were created. While Pix4D could do this automatically, manual creation of tie points was also implemented. There was one instance where the program struggled to create tie points for five images. In this case, manual tie points were created for those "error" images, ensuring accuracy and completeness in the overall reconstruction. Afterward, it underwent a calibration process that generated a dense point cloud (a set of 3D points that represent the model) and mesh (3D texture) of the data. Pix4D utilized the point cloud and mesh to generate index maps. This process involved analyzing pixels associated with each reflectance map, leading to the creation of blue, red, red-edge, and near-infrared data models. These models served as the foundation for calculating additional data models within Pix4D, such as the NDVI.

Ultimately, Vegetation Indices (VIs) can be derived from the five different bands, with numerous formulas available for various purposes, including soil analysis and plant quality assessment (Institute of Crop Science and Resource Conservation, 2023). For this study, four indices have been selected: the Normalized Difference Vegetation Index (NDVI) (Xie et al., 2007, p. 403), Normalized Difference Red Edge (NDRE) (Boiarskii, 2019, p. 2, pp. 25-27), Normalized Difference Water Index (NDWI) (Zarco-Tejada et al., 2003, p. 110), and Atmospherically Resistant Vegetation Index (ARVI) (Thenkabail et al., 2002, p. 615). These four VIs are chosen for their distinct advantages. NDVI and NDRE offer valuable insights into vegetation conditions, specifically chlorophyll content, as established in Section 3.2.2. The selection of NDWI and ARVI is influenced by the consideration of wet ground and rainfall conditions. NDWI is used to assess differences in wet soil. In contrast to NDVI, ARVI, while similar, provides the additional benefit of mitigating weather-related influences, thereby enhancing the reliability of the data. The following information and formulas are retrieved from the same source (Henricht et al., 2024): The NDVI, highlighting the disparity between the mesophyll content of the leaf and the presence of chlorophyll pigments, is calculated using the formula:  $NDVI = (NIR - RED) / (NIR + RED)$ . As the most accessible and widely used Vegetation Index (VI) in multispectral remote sensing, NDVI serves as a foundational reference. NDRE closely resembles NDVI but employs the RedEdge sensor, providing a more accurate measure of plants with lower chlorophyll content. Its calculation formula is:  $NDRE = (NIR - RedEdge) / (NIR + RedEdge)$ . NDWI utilizes the green and NIR bands to assess differences in wet soil and is calculated as:  $NDWI = (GREEN - NIR) / (GREEN + NIR)$ . Lastly, ARVI, similar to NDVI but capable of filtering out the effects of rain, air pollution, mist, and dust, is calculated using the formula:  $ARVI = (NIR - (2 * RED) + BLUE) / (NIR + (2 * RED) + BLUE)$ . These formulas were manually inputted into Pix4D, which then executed the calculations. Subsequently, these VIs are visually adjusted as GIS data models in GIS (QGIS) software for analysis. This facilitates colour adjustments to enhance differences and allows for layering and comparison of maps.

Based on Waagen (2023, pp. 14-15), the following procedure is described: the DJI Zenmuse L1 scanner captures LiDAR data in a proprietary DJI format (.LDR), which is then processed using DJI Terra (the free version). This processing involves creating a geolocated point cloud that includes

all recorded points and assigning colour intensity values using exported JPG images from the optical camera. The resulting dataset is exported in .LAS format to facilitate further analysis. To efficiently manage the point cloud, the free version of Rapidlasso GmbH LAStools is employed. This tool classifies the points, identifies ground points while excluding non-ground features like trees, ditches, and buildings, and generates individual digital terrain models (DTMs). The data is divided into 10x10 m tiles, with a maximum of 10,000 points per tile, resulting in a 1 centimetre resolution. Subsequently, the individual DTMs are consolidated into a single DTM using GIS software, specifically QGIS. In QGIS, the DTM can be visualized, and raster values can be displayed using a single band pseudo colour scheme. To enhance the visualizations for this project, the interactive local cumulative cut stretch toolset in QGIS is utilized.

To better analyse the GIS data models, experimentation with colours, contrasts, and brightness was done during this research. Such experimentation enables the detection of minimal differences that may not be visible at first glance. This is because the human visual system is unable to discern a difference of 2% in light intensity. In some cases, this percentage can even be higher. As a result, adjacent pixels with slightly different intensities may appear the same. Additionally, the human eye struggles to differentiate colours with minimal distinctions from each other, causing pixels close to each other to appear identical even when differences exist. Therefore, it is important to manipulate the visualisation of GIS data models during analysis, altering colours, contrasts, and intensity to perceive these differences when they are present (Emaus, 2022, p. 54). During the research, this was done by applying the twelve standard advised colour ramps from the single-band pseudo colour section in QGIS (Layer properties – Symbology), thereby adjusting the visualization.

### 3.5 Results and comparison

In this section, the results for each method employed in the 2023 study are outlined, including multispectral sensors, LiDAR sensors, and optical imagery. Following this, a section compares the three images with the findings from the thermal study conducted in 2019.

#### 3.5.1 Research results 2023, multispectral analysis

During the analysis of the multispectral data, the minimum expected pixel size was successfully achieved; 5,62 centimetres per pixel (appendix 2) allowing for a clear observation. The following observations were made: In Figure 13 (A), ditches in a rectangular formation can be observed and identified as plot boundaries, which were also recognized in the 2019 study. Additionally, clear traces from that excavation were prominently visible (B). These were distinctly noticeable during the study. These features were also apparent during the fieldwork and were clearly discernible on the multispectral data model (Figure 13, B)). To the east of the excavation remnants, there is a clearly discernible plot boundary running from north to south (Figure 14, C). Following this, there is a stretch of public road, seamlessly connected to another plot boundary. This boundary corresponds to a filled-in ditch. In the far east of the surveyed area, approximately thirty dots are visible, each with dimensions of approximately forty centimetres. These dots are arranged in a row, forming a crescent shape or "L" (Figure 15, D). The dimensions of this figure are approximately eighteen meters in length and ten meters in width, although it is hard to determine exactly what it is. In the northern part of the figure, the dots eventually cease to exist, while in the eastern part, there is a ditch and trees. Nonetheless, due to the explicit nature of this figure, it may still represent a potential archaeological feature.

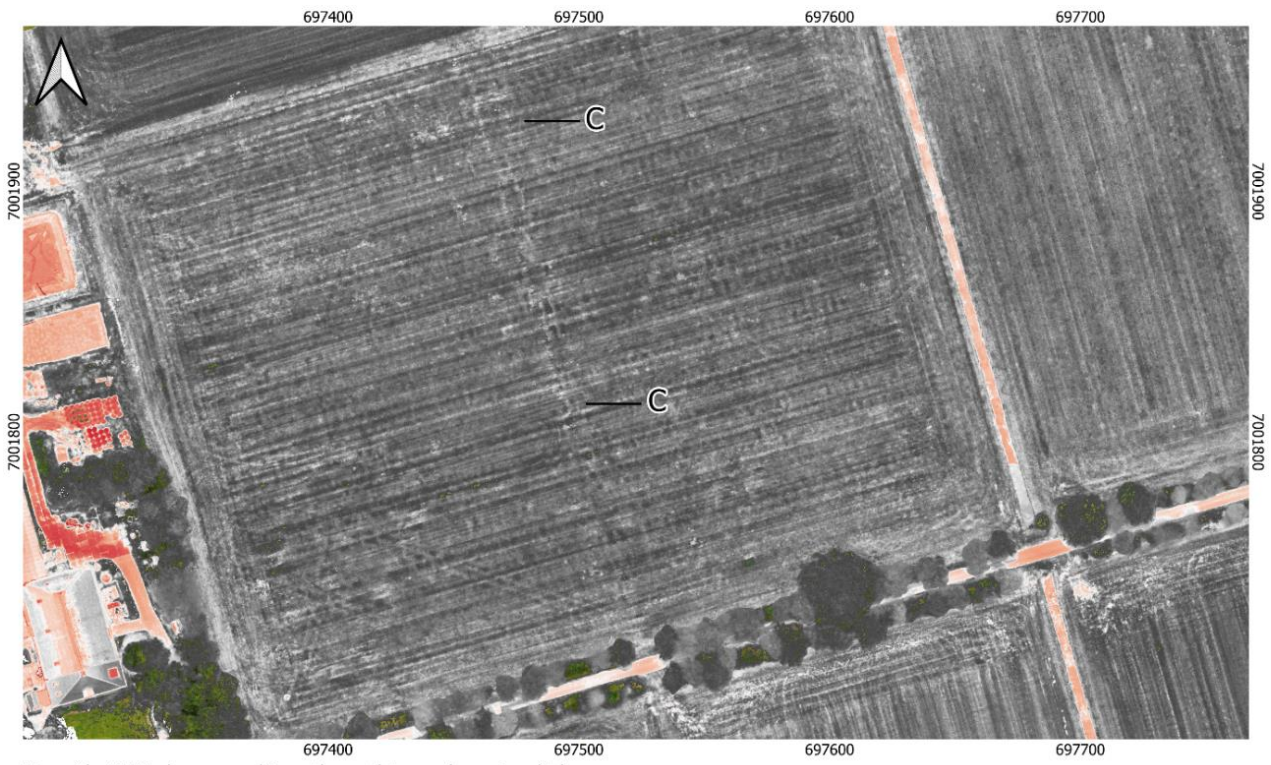


Map with ARVI index, zoomed in on the ditches arranged in a rectangular formation and excavations.



Kevin Hovens

Figure 14: multispectral data ARVI index, ditches in a rectangular formation (own work).



Map with ARVI index, zoomed in on the north to south-running ditch.



Kevin Hovens

Figure 13: multispectral data ARVI index, north to south-running ditch (own work).

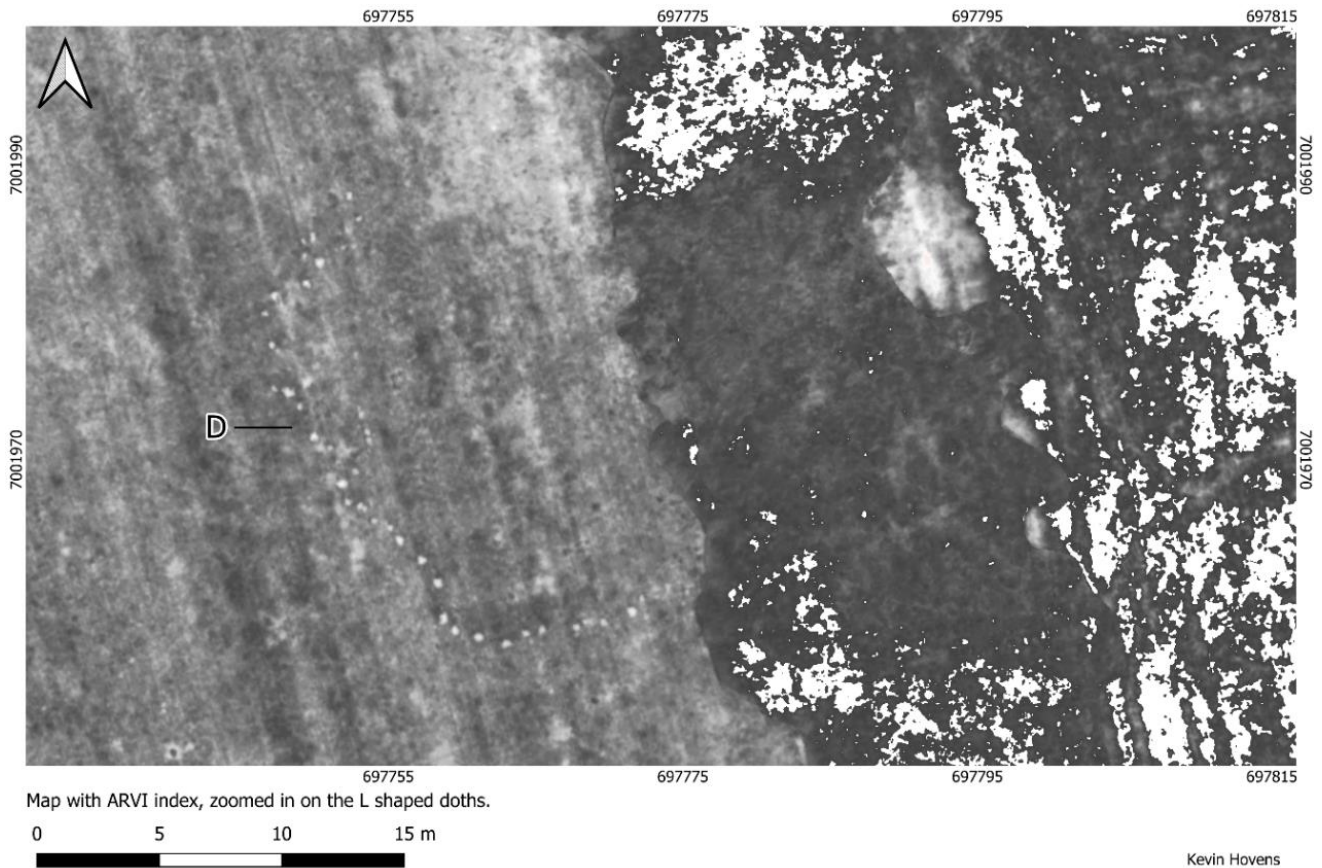


Figure 15: multispectral data ARVI index, L shaped doths (own work).

In Figures 13, 14, and 15, distinct lines from tractor tracks and fertilization can be observed. This can cause noise in the multispectral data model, making archaeological traces more challenging to recognize. Additionally, the identification of existing crop marks becomes more challenging, as these disturbances intersect with the crop marks, rendering them less distinguishable. Therefore, it can be assumed that agricultural activities impacted the results. During the analysis, the four VIs (Vegetation Indices) mentioned were utilized: NDVI, NDRE, NDWI, and ARVI. Similar findings were observed on all these maps, with the features on the NDWI being the least visible. Furthermore, it was particularly interesting to examine ARVI and NDVI, especially due to the rainfall that was supposedly filtered out during the observation. The difference between the two indices was minimal, making it inconsequential which one was used during the analysis. The primary distinction arose from the use of the colour slider, as explained in Section 3.4.3.

### 3.5.2 Research results 2023, LiDAR analysis

During the analysis of the LiDAR data, the minimum expected pixel size was successfully achieved; 5 centimetres per pixel (appendix 2) allowing for clear observation. The GIS data models produced by the LiDAR sensors offer several noteworthy observations. In the western section of the study area, a ditch in the shape of a rectangle can be observed, which aligns with the visual findings from the fieldwork (Figure 16, A). These variations in elevation stand out noticeably, underscoring their clarity. Additionally, the anticipated disturbances resulting from the 2019 excavations are visible but challenging to discern (Figure 16, B). Upon shifting focus to the eastern side of the ditches (Figure 16, A), an elongated, filled-in ditch extending from north to south comes into view (Figure 16, C). It extends beyond this parcel into another area where it

remains in an unfilled state. Furthermore, situated at the heart of the study area, one can observe a set of scattered lines oriented from the northeast to the southwest. These lines may potentially represent historical plot boundaries. Some of these lines intersect with others of varying orientations, where in the southernmost part, a rectangle is formed. (Figure 16, E). These lines and configurations are aligned with the rectangular ditches (Figure 16, A). In the eastern segment of the study site, a square-shaped feature becomes apparent. Its extension into the wooded area and its convergence with the adjacent ditch present an intriguing puzzle. While it may suggest some form of man-made construction, precisely categorizing its origin proves to be a challenging task. It could potentially be a natural phenomenon, such as molehill activity. The visible portion of this feature, extending up to the ditch and tree boundary, spans roughly seventeen by fourteen meters (Figure 17, D). In Section 3.5.3, the optical data model indicates that these are likely molehills. Finally, the agricultural influences are distinctly evident. The presence of manure injection lines, tractor tracks, and ploughing marks is strikingly pronounced.

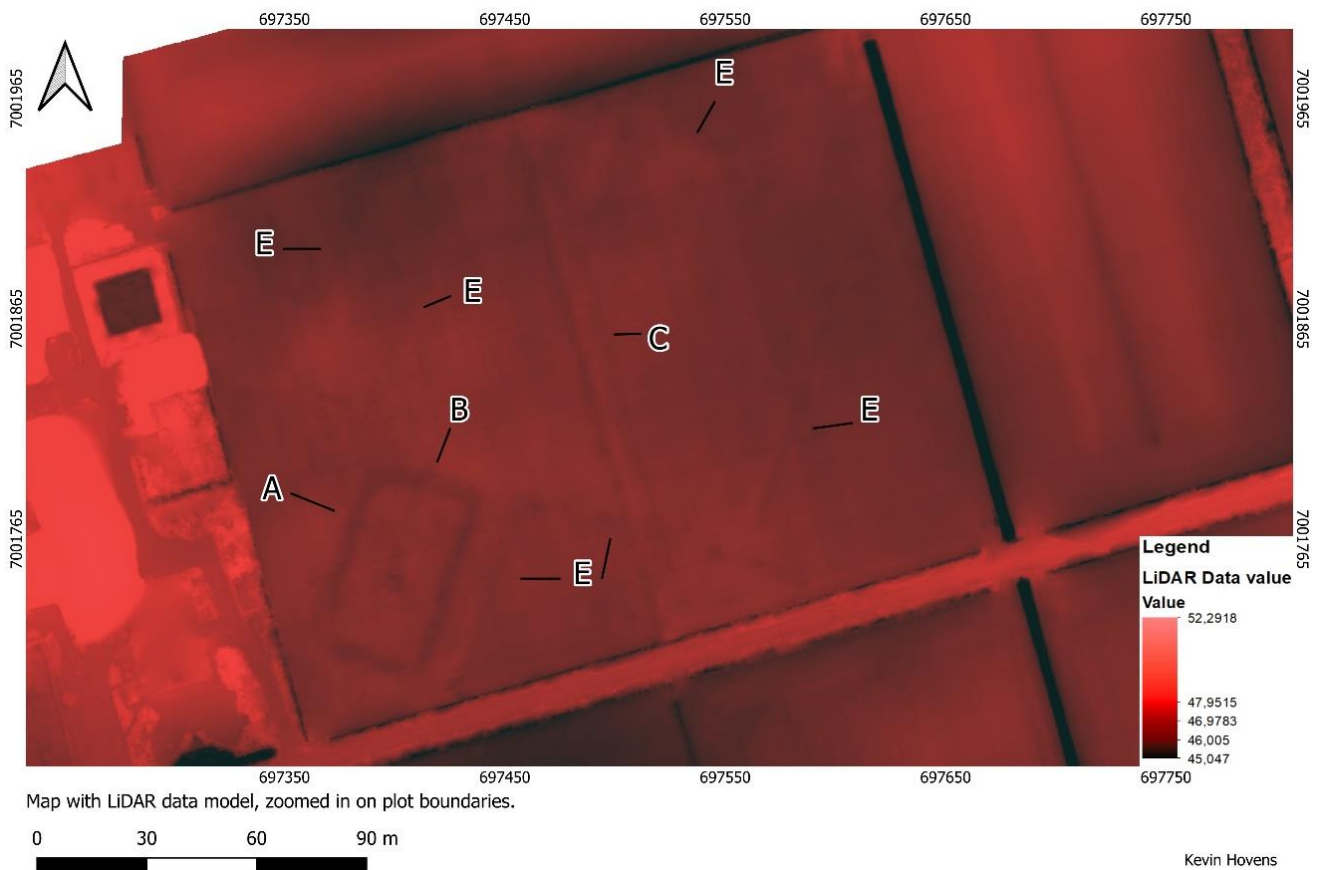
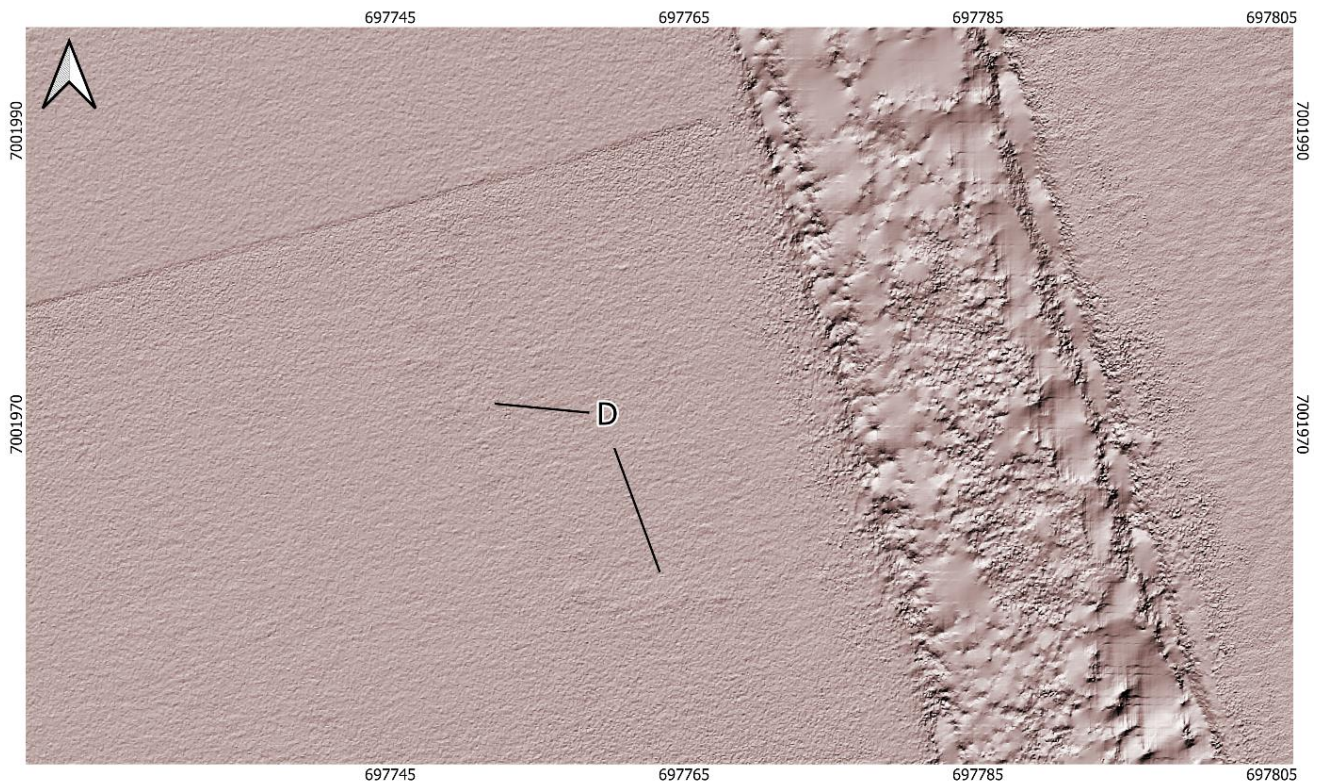


Figure 16: LiDAR data model, plot boundaries, excavation remnants (own work).



Map with Lidar data model, with hillshade render, zoomed in on the L shaped figure.



Kevin Hovens

Figure 17: LiDAR data, L shaped figure (own work).

### 3.5.3 Research results 2023, optical image

Based on information from QGIS, the pixel size of the optical data model is 1.91 centimetres per pixel (Layer properties - Information - Pixel Size). This confirms that the minimum expected pixel size has been achieved, allowing for a clear comparison. The optical image serves as a tool to compare the identified features from multispectral and LiDAR images with real-world visuals, enabling the discernment of whether these features are of natural, human-made, or contemporary origin within the landscape. Beginning with an examination of the features in the western sector of the research area, we encounter a ditch in the shape of a rectangle. Additionally, the remnants from the 2019 excavation are still evident in this vicinity. As we progress eastward, we come across a clearly visible filled-in ditch that runs from north to south, extending onto another parcel where it remains unfilled. Further to the east of the study area, a square/L-shaped figure can be identified. Upon closer inspection, these are black mounds of soil, indicative of what appears to be molehills (Figure 18). While the aerial photograph might not offer the clearest view, this would be the most plausible explanation in this case. Nevertheless, it remains a peculiar figure with a consistently large accumulation of mounds. The unnatural appearance suggests that the mole might be digging around an object or structure in the soil. Lastly, the images distinctly reveal the traces of agricultural activities on the landscape.



Figure 18: optical data, zoomed dots (own work).

### 3.5.4 Comparison between the 2019 and 2023 research

When comparing the data from 2019 to that of 2023, several noteworthy points come to light. In Figure 19, an overview is provided showcasing the visibility of the defined features per data model. Firstly, the area covered during the 2023 data collection is considerably larger, nearly three times the size compared to the thermal infrared data collection from 2019. This is important because, for the 2023 research, the landowner had mowed a much larger portion of grassland compared to the research conducted in 2019. In the areas common to both datasets, several observations stand out. Both datasets clearly depict ditches that form a rectangle on the terrain. In Section 3.1.6, a figure within the rectangle is mentioned (Figure 6, F). This figure is only visible in the thermal infrared data model. On the multispectral, optical and LiDAR data models, it is no longer visible due to the remnants of the 2019 excavation. Instead, remnants of the excavation are present. Importantly, these remnants are almost imperceptible on the LiDAR data model. Furthermore, the north-south oriented ditch is clearly visible on the multispectral, LiDAR, and optical images from 2023 and the thermal-infrared images from 2019. One particularly interesting observation pertains the scattered plot boundaries that are clearly visible on the LiDAR data model. Some of these lines are also visible on the thermal data model. However, on the multispectral data model, they are almost invisible and only stand out because they were detected on the LiDAR and thermal data models. This is likely due to the conditions during the data acquisition, which included constant rain, overcast skies, the absence of vegetation stress, and disturbance from agriculture. LiDAR and thermal data are less affected by these factors, except for weather conditions, making the lines more visible. In the east of the research area, there is a figure that can be recognized. This figure is beyond the research area from the 2019 images. Therefore, the new data cannot be compared with old data. Therefore, a

comparison will be made between the multispectral, LiDAR, and optical images. On the multispectral data, we can see clear spots in an L-figure. When we look at the LiDAR data, we can measure the heights of these spots. There is a clear height difference between the spots and the environment. When looking at the optical images, these are black sandy slopes. Therefore, examining the three images suggests that the most likely outcome relates to molehills. Finally, the noise originating from agricultural activities is notably less intrusive in the analysis of thermal remote sensing data models compared to multispectral and LiDAR data models. This is because agricultural activities have a significant impact on vegetation, such as flattening and fertilization, promoting better growth (Section 3.3). Multispectral data models focus on vegetation, making agricultural activities highly visible. In the case of LiDAR, it only applies when earthworks are created, so the activities are visible but to a lesser extent.

Figure 19:

Table indicating the visibility of the defined features per data model

	<i>Thermal infrared sensor 2019</i>	<i>Multispectral sensor</i>	<i>LiDAR sensor</i>	<i>Optical sensor</i>
<i>Rectangular plot boundary (A)</i>	well-visible	well-visible	well-visible	well-visible
<i>2019 excavation remnants (B)</i>	absent	well-visible	poorly visible	well-visible
<i>north to south running ditch (C)</i>	well-visible	well-visible	well-visible	well-visible
<i>L shaped dots (D)</i>	outside the perimeters of the data model	well-visible	moderately visible	well-visible
<i>Scattered plot boundaries (E)</i>	well-visible	poorly visible	well-visible	poorly visible
<i>Rectangle (F)</i>	Well visible	Absent	Absent	absent
<i>Agricultural activities</i>	poorly visible	well-visible	Moderately visible	Moderately visible

Figure 19: Table showcasing the visibility of the defined features per data model (own work)

## 4. Conclusion

### *1. What is multispectral remote sensing?*

Multispectral remote sensing is a technology that captures data at various wavelengths across the electromagnetic spectrum. This involves utilizing sensors capable of detecting specific bands, such as Green, Red, Blue, and near-infrared. In practical terms, this technique allows for the collection of information about the Earth's surface or other objects by analyzing the reflected or emitted electromagnetic radiation within these predefined spectral bands from a distance .

### *2. How can crop marks be recognized using multispectral data?*

Crop marks can be recognized using multispectral data by analysing the reflectance patterns of crops in different spectral bands. Multispectral sensors capture data in multiple bands; Green, Red, Blue, near-infrared, and red-edge. The variation in reflectance values across these bands can highlight different characteristics of vegetation, making crop marks distinguishable.

### *3. What types of vegetation are present at the research site in Siegerswoude?*

Identifying the vegetation proved to be a challenge in the study. The site turned out to be an old grassland that has remained unchanged for thirty years. As a result, the grassland is characterized by a mixture of grass and herb species.

### *4. What is the soil composition at the research site in Siegerswoude?*

Examining the geomorphology of the reagon, the research area is situated in a terrain of "grondmorenenwieling." This glacial deposition occurs when land ice transports material underneath the ice, creating undulating soil. It contains a layer of "keileem," a type of soil consisting of sand, clay, loam, and rocks. The previously mentioned "keileem" in the Siegerswoude region is generally covered with "podzol" soils. In the case of this region, this indicates that the subsoil layer (B-horizon) consists exclusively of humus. In the research area, there is only one soil type: "Veldpodzol soil, characterized by loamy and weakly loamy fine sand." This suggests that there was a period when a peaty layer was present on top of this soil.

The excavation from 2019 shows that in the designated area, the soil profile is characterized by an A-horizon, displaying features resembling a B/E-horizon, with a modest amount of artificially introduced loam. The natural substrate (C-horizon) consists of light brown sand with minimal gravel content, transitioning to prevalent loam at a depth of sixty centimetres. The groundwater level in the research area fluctuates seasonally, ranging from a minimum depth of forty-five centimetres beneath the surface to an average maximum depth of 150 centimetres beneath the surface, with an average depth of sixty centimetres beneath the surface during the spring season.

### *5. What are the expected findings that may be observed during the analysis of the new data models based on the research activities from 2019 in Siegerswoude?*

As explained in Section 3.1.6, an arrangement of plot boundaries is anticipated. These plot boundaries may result in crop marks and earthworks. Consequently, the decision was made to utilize multispectral and LiDAR sensors.

*6. What are the requirements for obtaining high-quality data during the multispectral remote sensing research in Siegerswoude?*

By utilizing the information provided by expert Dr. J. Waagen, the research question was successfully concluded, resulting in high-quality data. This is because the data possessed sufficient quality for a thorough analysis, as evidenced in sections 3.5.1, 3.5.2, and 3.5.3. Additionally, there was an expectation of a pixel size of 17 centimetres per pixel. Ultimately, this turned out to be 5.62 cm/pixel for the multispectral data, 5 cm/pixel for the LiDAR, and 1.91 cm/pixel for the optical data. More information about data acquisition and processing can be found in Appendices 1 and 2.

*7. How does the expected findings based on the 2019 research in Siegerswoude differ from the observations obtained from the multispectral data?*

Comparing the 2019 and 2023 data reveals several key findings. The 2023 dataset covers a significantly larger area, about three times the size. Common areas in both datasets show ditches arranged in a rectangular formation (plot boundaries). Remnants of the 2019 excavation are clearly visible in the multispectral and optical data. However, the excavations are almost not visible in the LiDAR data. As predicted, figures of plot boundaries will be seen on the data models. The plot boundaries in the research area are clearly visible on the LiDAR and thermal data model but are almost invisible on the multispectral data. In the east of the research area, an L-shaped figure is observed. Comparing multispectral, LiDAR, and optical images suggests these are likely molehills.

Main research question:

*What is the impact of vegetation stress on the detection of archaeological traces through multispectral remote sensing in Siegerswoude?*

This research has revealed that multispectral sensors can effectively capture subtle variations in vegetation stress. Archaeological features within the research area in Siegerswoude have been identified through the application of multispectral sensors, as illustrated in Figure 19. This emphasizes that the impact of vegetation stress on the detection of archaeological traces through multispectral remote sensing is substantial. Notably, these observations were made under less-than-ideal weather conditions when optimal differences in vegetation stress might not be present. This underscores the significant potential of multispectral analysis for archaeological prospection. Despite the capability of multispectral sensors to unveil archaeologically relevant crop marks, it's worth noting that, in this particular case, superior results were achieved using LiDAR sensors.

## 5. Discussion/Reflection

In general, the initially drafted research plan was largely adhered to during the investigation, with some adjustments made. Initially, the plan was to produce a report in 4D-lab format for the University of Amsterdam, accompanied by an accountability document. However, it was later realized that this format closely matched the thesis requirements of Saxion University of Applied Sciences. Consequently, in consultation with Dr. J. Waagen and R. Emaus, the decision was made to proceed with writing a thesis. Initially, the plan was to collect only multispectral sensor data. However, considering that we were already going to the research location, the decision was made to also employ other sensors, such as LiDAR and a Thermal Infrared sensor. This decision was partly inspired by a similar study conducted by the 4D-lab in 2022 (Waagen, 2023). Another modification was related to the initial choice not to compare the data from the current research with the thermal infrared research from 2019. Eventually, this comparison was conducted in Chapter 3.5.4, as it seemed logical to address this aspect in one paper instead of multiple papers. Furthermore, several side products were initially planned to be created alongside the thesis, including a Personal Geodatabase, GIS raster files rendered from Pix4D, various maps based on the GIS raster data, a flight plan, orthophotos, and metadata. However, two changes were implemented. First, the flight plan is now considered confidential and will not be published. Second, it was determined that there was no necessity to create a Personal Geodatabase for the results, and this was consequently omitted. Additionally, a sub-question was adjusted. The original sub-question 5, "What are the expectations in Siegerswoude based on the research conducted in 2019?" was not sufficiently clear in expressing the expectations. Hence, a new sub-question was formulated: "What are the expected findings that may be observed during the analysis of the new data models based on the research activities from 2019 in Siegerswoude?" Finally, one sub-question remained unanswered. Sub-question 3, "What types of vegetation are present at the research site in Siegerswoude?" was left unanswered due to a lack of specialization. A specialist with the appropriate equipment would be needed to identify specific plant species. Consequently, the results were not linked to specific plant types and their characteristics. Overall, even with the changes, the research was successfully completed with results.

It is also vital to evaluate how this research could have been conducted more effectively. As mentioned, challenging weather conditions affected the drone flights, and the individual schedules limited flying opportunities. Ideally, flights should have been conducted during periods of dry weather with strong sunlight, but this was not possible. Additionally, the thermal-infrared flight, which was initially planned but later changed due to weather conditions, was never executed. A more optimal scenario would involve flying at various times in different seasons with the same sensors to capture different environmental conditions, similar to the Weesp project (Waagen, 2023). However, within the scope of this project, that was not feasible. Additionally, it would be valuable to compare the findings with a similar location but with a vastly different soil composition, yet the same vegetation or a location with entirely different vegetation but matching soil composition, where it is known that crop marks exist. This would allow for an examination of the effects of stress under similar and varying conditions. During this research, there was no basis for such comparisons except with other remote sensing techniques, rendering a comparison unfeasible. The aforementioned approach would undoubtedly require a significant amount of time, funding, and resources. The 4D lab of the University of Amsterdam focuses on that task. Given the constraints of completing this research within a 20-week timeframe, such an extensive comparison was not feasible.

Determining why the plot boundaries are less visible in multispectral data is challenging. It could be influenced by agricultural practices, extensive land use, or alterations to the landscape, which may have resulted in an overall consistent ground structure. This could imply that even if the vegetation experiences stress, it may not be significantly affected by the underlying characteristics due to the largely consistent soil structure in the study area. Moreover, the nature of the plant itself could play a substantial role in this context. Grass, as mentioned earlier, has minimal foliage and shallow roots. This means that the underlying traces may not influence the grass landscape, at least not significantly in the relevant areas. When considering these factors, the conclusion is rather clear. As discussed in previous Sections, in the field of archaeological prospection, the outcomes depend on a multitude of factors. These include weather conditions, which posed numerous challenges during the 2023 fieldwork, as well as land use, soil composition, vegetation, equipment, and the potential types of archaeological traces present.

What is interesting is the fact that on the LiDAR data model, the remnants of the excavations are almost invisible. However, all other structures that are much less recent are very well visible. The opposite happens with the multispectral data. There, the excavation remnants are clearly visible, while the remaining structures are less visible to almost invisible. So, in the multispectral data model, the old traces are less visible than the new ones, and with LiDAR, this is precisely the opposite. This could be due to the weather situation and the lack of vegetation stress, thereby affecting the multispectral data model.

## 6. Recommendations

Based on this research, it is recommended to revisit Siegerswoude in different periods and under various weather conditions. This approach allows for a comprehensive comparison between different sensors and their data models. An additional benefit is that multiple multispectral data models will be generated from different periods and weather conditions from the same research area. This will result in a more comprehensive and reliable conclusion concerning the main research question.

While this study successfully employed a high-end drone, demonstrating its effectiveness in adverse weather conditions and producing valuable results, the potential influence of different weather conditions on the outcomes remains uncertain. It is recommended to conduct further research specifically addressing the impact of diverse weather scenarios on remote sensing measurements, taking into consideration the variations in equipment quality from low-end to high-end. This additional investigation will provide insights into how different weather conditions may affect the performance of various equipment deviations, contributing to a more comprehensive understanding of the role played by different equipment types in remote sensing measurements and their resulting outcomes.

Finally, based on the findings of this research, it is strongly recommended to adopt a comprehensive approach that involves the integration of multiple remote sensing techniques when using remote sensing. While individual sensors, such as thermal or multispectral, provide valuable data, the synergy achieved through combining them enhances the overall effectiveness of the study. This research emphasizes that the absence of LiDAR or thermal sensors could lead to the oversight of crucial features, such as plot boundaries, in multispectral data. Following the example set by the 4D Lab at the University of Amsterdam, researchers are encouraged to explore and implement multidisciplinary approaches that combine various remote sensing techniques, as highlighted in Waagen (2023). This collaborative approach will provide a more nuanced and comprehensive insights into archaeological features and landscapes during remote sensing analysis.

## Bibliography

- Casana, J., Wiewel, A., Cool, A., Hill, A. C., Fisher, K. D., & Laugier, E. J. (2017). Archaeological Aerial Thermography in Theory and Practice. *Advances in Archaeological Practice*, 5(4), 310-327.  
<https://doi.org/10.1017/aap.2017.23>
- Cool, A. C. (2018). Thermography. In S. L. López Varela (Red.), *The Encyclopedia of Archaeological Sciences* (pp. 1-5). John Wiley & Sons, Inc.  
<https://doi.org/10.1002/9781119188230.saseas0579>
- Cropx. (2023, November). *Boer&Bunder*. Retrieved from Boer&Bunder: <https://boerenbunder.nl/>
- DJI Enterprise. (2022, July 28). *LiDAR Drone Systems: Using LiDAR Equipped UAVs*. Retrieved from DJI Enterprise: <https://enterprise-insights.dji.com/blog/lidar-equipped-uavs>
- Doesburg, J. van, Heiden, M. van der, Waagen, J., Os, B. J. H. van, & Meer, W. van der. (2022). *Op zoek naar lijnen: De waarde van elektromagnetische inductie en optische en thermische infraroodbeelden in Siegerswoude (Friesland)*. Rijksdienst voor het Cultureel Erfgoed.
- Eitel, J. U. H., Höfle, B., Vierling, L. A., Abellán, A., Asner, G. P., Deems, J. S., Glennie, C. L., Joerg, P. C., LeWinter, A. L., Magney, T. S., Mandlbürger, G., Morton, D. C., Müller, J., & Vierling, K. T. (2016). Beyond 3-D: The new spectrum of lidar applications for earth and ecological sciences. *Remote Sensing of Environment*, 186, 372-392.  
<https://doi.org/10.1016/j.rse.2016.08.018>
- Emaus, R. (2022). Beeldoptimalisatie en interpretatie van analoge luchtfoto's. In E. Rensink, E. M. Theunissen, & H. Feiken (Red.), *Vanuit de lucht zie je meer: Remote sensing in de Nederlandse archeologie* (pp. 53-57). Rijksdienst voor het Cultureel Erfgoed.
- ESRI. (2024, January). *GIS Dictionary*. Retrieved from ESRI : <https://support.esri.com/en-us/gis-dictionary/orthophotograph>
- Henrich, V., Krauss, G., Götze, C., & Sandow, C. (2012). *List of available Indices*. Retrieved from Index Database: <https://www.indexdatabase.de/db/i.php>

Institute of Crop Science and Resource Conservation. (2023, oktober). *List of available Indices*.

Retrieved from Index DataBase: <https://www.indexdatabase.de/db/i.php>

James, K., Nichol, C. J., Wade, T., Cowley, D., Gibson Poole, S., Gray, A., & Gillespie, J. (2020).

Thermal and Multispectral Remote Sensing for the Detection and Analysis of

Archaeologically Induced Crop Stress at a UK Site. *Drones*, 4(4), 61.

<https://doi.org/10.3390/drones4040061>

Lascaris, M., & Os, B. J. H. van. (2019). Effecten van agrarische grondbewerking op archeologie. In

M. Lascaris, B. J. H. van Os, & R. C. G. M. Lauwerier (Red.), *Archeologie en verstoring door*

*bodembewerkingen: Evaluatie van de effecten van grondbewerking in agrarisch en*

*stedelijk gebied en het onderzoek daarnaar*. Rijksdienst voor het Cultureel Erfgoed.

Lascaris, M., Os, B. J. H. van, & Lauwerier, R. C. G. M. (Red.). (2019). *Archeologie en verstoring door*

*bodembewerkingen: Evaluatie van de effecten van grondbewerking in agrarisch en*

*stedelijk gebied en het onderzoek daarnaar*. Rijksdienst voor het Cultureel Erfgoed.

Kadaster. (2003). *Dataset: BRO Geomorfologische kaart (GMM)*. Retrieved from pdok:

<https://www.pdok.nl/introductie/-/article/bro-geomorfologische-kaart-gmm->

Kadaster. (2022, January 1). *Dataset: BRO bodemkaart (SGM)*. Retrieved from pdok:

<https://www.pdok.nl/introductie/-/article/bro-bodemkaart-sgm->

Maas, G., van der Meij, W., Delft, S., & Heidema, H. (2021). *Toelichting bij de legenda*

*Geomorfologische kaart van nederland 1:50 000 (2021)*. Retrieved from Geomorfologische

kaart van Nederland 1:50 000 (2021): <http://legendageomorfologie.wur.nl/>

National Aeronautics and Space Administration. (2013, March). *Imagine The Universe*. Retrieved

from NASA: <https://imagine.gsfc.nasa.gov/science/toolbox/emspectrum1.html>

orlando, P., & Villa, B. (2011). Remote sensing applications in archaeology. *Archeologia e*

*Calcolatori*, 22, 147-168.

Pix4D. (2023, November). *Photogrammetry knowledge*. Retrieved from Pix4D:

<https://support.pix4d.com/hc/en-us/sections/360000212943-Photogrammetry-knowledge>

- Raj, T., Hashim, F. H., Huddin, A. B., Ibrahim, M. F., & Hussain, A. (2020). A Survey on LiDAR Scanning Mechanisms. *Electronics*, 9(5), 741. <https://doi.org/10.3390/electronics9050741>
- Remmelink, G., van Middelkoop, J., Ouweltjes, W., & Wemmenhove, H. (2020). Grasland en voedergrassen. In G. Remmelink & LR - Animal Nutrition, *Handboek melkveehouderij 2020/21* (pp. 90-129). Wageningen Livestock Research. <https://doi.org/10.18174/529557>
- Rensink, E., Theunissen, L., Feiken, H., van Doesburg, J., van der heiden, M., Jansen, D., & de Kort, J. W. (2022). *Archeologische prospectie vanuit de lucht. Remote Sensing in de Nederlandse archeologie (landbodems)* (programma Kennis voor Archeologie, pp. 1-97).
- Rijkswaterstaat Bodem+. (2023, 15 9). *Agendering grondwaterbelangen*. Retrieved from bodemplus: <https://www.bodemplus.nl/onderwerpen/bodem-ondergrond/grondwater/grondwater-ro/agendering/>
- Schotanus, B. (1718). *Opsterland in de atlas van schotanus 1698* [Map]. Friese Staten.
- Scollar, I., Tabbagh, A., Hesse, A., & Herzog, I. (2009). *Archaeological prospecting and remote sensing* (Digitally printed version). Cambridge University Press.
- Smit, B., & Jager, J. (2023). *Schets van de akkerbouw in Nederland: Structuur-, landschaps- en milieukeurmerken die een relatie hebben tot biodiversiteit* (Nr. 2018-074; Wageningen Economic Research notitie, p. 33). Wageningen Economic Research; [edepot.wur.nl/463816](https://edepot.wur.nl/463816)
- Steur, G. G. L., & Heijink, W. (1972). Moerige gronden in Nederland. *BOOR en SPADE*, 18, 9-40.
- Štroner, M., Urban, R., & Línková, L. (2021). A New Method for UAV Lidar Precision Testing Used for the Evaluation of an Affordable DJI ZENMUSE L1 Scanner. *Remote Sensing*, 13(23), 4811. <https://doi.org/10.3390/rs13234811>
- TNO Geologische Dienst Nederland. (2023). *Ondergrondgegevens*. Retrieved from [DINOloket: https://www.dinoloket.nl/ondergrondgegevens](https://www.dinoloket.nl/ondergrondgegevens)
- TNO Geologische Dienst Nederland. (2023a, October). *Laagpakket van Gieten*. Retrieved from [DINOloket: https://www.dinoloket.nl/stratigrafische-nomenclator/laagpakket-van-gieten](https://www.dinoloket.nl/stratigrafische-nomenclator/laagpakket-van-gieten)

TNO Geologische Dienst Nederland. (2023b, September). *Ondergrondmodellen*. Retrieved from

[DINOloket: https://www.dinoloket.nl/ondergrondmodellen/kaart](https://www.dinoloket.nl/ondergrondmodellen/kaart)

TNO Geologische Dienst Nederland. (2023c). *Formatie van Boxtel; Laagpakket van Wierden*.

Retrieved from DINOloket: <https://www.dinoloket.nl/stratigrafische-nomenclator/laagpakket-van-wierden>

Waagen, J. (2023). *4DRL Report Series 4 - In search of a castle: Multisensor UAS research at the Medieval site of 't Huijs ten Bosch, Weesp*. 40394639 Bytes.

<https://doi.org/10.21942/UVA.23375486>

Waagen, J., Sánchez, J. G., van der Heiden, M., Kuiters, A., & Lulof, P. (2022). In the Heat of the Night: Comparative Assessment of Drone Thermography at the Archaeological Sites of Acquarossa, Italy, and Siegerswoude, The Netherlands. *Drones*, 6(7), 1-21.

<https://doi.org/10.3390/drones6070165>

Wageningen University & Research. (2023). *Wageningen University & Research Unmanned Aerial Remote Sensing Facility (UARSF)*. Retrieved from Wageningen University & Research:

<https://www.wur.nl/en/research-results/chair-groups/environmental-sciences/laboratory-of-geo-information-science-and-remote-sensing/research/integrated-land-monitoring/uarsf.htm>

Wallinga, J. (2020, October). *EARTHWORK project connects the past, present and future*. Retrieved

from Wageningen university & research: <https://www.wur.nl/en/newsarticle/earthwork-project-connects-the-past-present-and-future.htm>

Willemse, N. W. (2020). *Beschermd maar kwetsbaar: Fysieke bedreigingen van archeologische rijksmonumenten en maatregelen om ze te behouden*. Rijksdienst voor het Cultureel Erfgoed.

Worst, D. (2012). *Agrarische veenontginningen in oostelijk Opsterland (900—1700 AD)*

[Unpublished master's thesis]. University of Groningen, Letteren.

Worst, D., & Zomer, J. (2011). *Landschapsontwikkeling en cultuurhistorische waarden langs de boven- en middenloop van het Koningsdiep (Zuidoost-Friesland)* (Rapport nr. 1; p. 63).  
Rijksuniversiteit Groningen/Kenniscentrum Landschap.

## glossary

AD	Anno Domini (After the birth of Christ)
AHN	Dutch elevation map (Algemeen hoogtebestand Nederland)
ARVI	Atmospherically Resistant Vegetation Index
DTM	Digital Terrain Model
EES	Earth and Ecological Sciences (EES)
EM	Electromagnetic spectrum
GPS	global Positioning System
LiDAR	Light Detection of Laser Imaging And Ranging
LRI	laser return intensity
LDR	Lego Design File
mm	millimetre
NDRE	Normalized Difference Red Edge
NDVI	Normalized Vegetation Index
NDWI	Normalized Difference Water Index
PiX4D	Software platform specialized in processing aerial photos and drone images.
QGIS	Quantum Geographic Information System (open source software)
RCE	Cultural heritage Agency of the Netherlands (Rijksdienst voor het Cultureel Erfgoed)
tiff	Tagged Image File Format
UvA	University of Amsterdam
VI	Vegetation Index
2D	two-dimensional
3D	three-dimensional

### *Veldpodzol soil; loamy and weakly loamy fine sand:*

A veldpodzol occurs in sandy, nutrient-poor, periodically wet areas (Zijverden & Moor, 2014, p. 105) above "keileemplateaus" (a mixture of sand, clay, loam and rocks). It is characterized by a subsoil layer (B-horizon) consisting exclusively of humus (Zijverden & Moor, 2014, p. 108).

### *Veldpodzol soil; loamy fine sand:*

A veldpodzol occurs in sandy, nutrient-poor, periodically wet areas (Zijverden & Moor, 2014, p. 105) above "keileemplateaus" (a mixture of sand, clay, loam and rocks). It is characterized by a subsoil layer (B-horizon) consisting exclusively of humus (Zijverden & Moor, 2014, p. 108).

### *Laarpodzol soil; loamy fine sand:*

On the highest and driest areas of "keileemplateaus" (a mixture of sand, clay, loam, and rocks), there are so-called "haarpodzolgronden," which are similar to "veldpodzol." On top of the "haarpodzol," a man-made soil layer rich in humus, called "laarpodzol" soils, can be recognized (Zijverden & Moor, 2014, p. 110).

### *Vlierveen soil (peat soil) on sand without humus podzol, starting shallower than 120 cm.:*

Peat soil without podzol.

### *Moerige eerdgronden with a moerige topsoil on sand:*

"Moerige eerdgronden" are characterized by a sandy subsoil, with a surface layer or intermediate layer of less than 40 cm of peat. They represent the transition from peat soils to mineral soils (Steur & Heijink, 1972, p. 4).

*Moerige eerdgronden with a sand cover and a moerige intermediate layer of sand:*

"Moerige eerdgronden" are characterized by a sandy subsoil, with a surface or intermediate layer of less than 40 cm of peat. They represent the transition from peat soils to mineral soils (Steur & Heijink, 1972, p. 4).

## Appendix 1: data capture parameters

<b>Project planning</b>	Title	Middenwei, Siegerswoude
	Brief description	Grass site examination
	Purpose	Determine state, type and extent of subsoil remains
	Platform	Multirotor
	Date of flight(s)	21-09-2023
	Operator	UvA Dronelab (4DRL)
	Pilot in Command	Jitte Waagen
	Observers	Kevin Hovens

### Multispectral survey

<b>System calibration</b>	Sensor type	Multispectral, 4/3"
	Scanner/camera model	Micasense Rededge
	Centre bandwidths	B (475), G (560), R (668), RE (717), NIR (840)
	Lens	5.4mm
	Shutter type	Global (all sensors)
	Instruments	DJI M300, Geomax Zenith15 dGPS, Downwelling Light Sensor 2
	Pixels	1.2MP (all sensors)
	Precision	1280x960 (all sensors)
	Accuracy	N/A
<b>Data acquisition</b>	Time	13.28
	Exposure triangle	Automated
	Altitude Above Ground Level	80m
	Average Speed	3,3m/s
	Overlap (side- and front)	80/70%
	Estimated type archaeology	ditches
	Estimated depth archaeology	10-100cm
	Vegetation type	Grassland
	Vegetation state	Recently moan

	Moisture conditions	Intermitted very light rain
	Superficial layer	Loam on Sand
	Soil matrix	Loam on Sand
	Light conditions	Overcast
	Number of photos	2990
	Format	TIF
<b>Geometric correction</b>	Flight trajectory calculation (software/method)	DJI Pilot/grid
	GCPs used	16
	GCP geolocation instrument	Geomax Zenith15, 06GPS
	GCP geolocation accuracy	1-2cm
	GCP and photo merging	Pix4D
	Coordinate system	Amersfoort/RD New (EGM 96 Geoid), EPSG: 28992
<b>Radiometric correction</b>	Downwelling Light Sensor used	yes
	Calibration reflectance panel	yes
	Processing and calibration	Pix4D
	Setting	Camera, Sun Irradiance and Sun Angle using DLS IMU

### LiDAR survey

<b>System calibration</b>	Sensor type	Discrete-return LiDAR
	Scanner/camera model	Zenmuse L1, Livox LiDAR module
	Instruments	DJI M300, D-RTK 2 Mobile Station
	Pulse repetition rate	240 kHz in 2 return mode, 160 kHz in 3 return mode
	Wavelength	905nm
	Point rate	Multiple return: max. 480.000pts
	Additional sensors	Optical camera (20 MP, 4864x3648 (4/3"), 8.8mm, Global shutter)
	Accuracy (max. scanning angle error)	Horizontal: 10cm @ 50m; Vertical: 5cm @50 m

	INS angle accuracy	Yaw Accuracy (RMS 1 $\sigma$ ): Real-time: 0.3°, Post-processing: 0.15° Pitch/Roll Accuracy (RMS 1 $\sigma$ ): Real-time: 0.05°, Post-processing: 0.025°
	INS-GNSS-laser synchronisation error	N/A
<b>Data acquisition</b>	Time	14:20
	Altitude Above Ground Level	70m
	Average Speed	5m/s
	Swath width	30m
	Flight strip overlap	50%
	Footprint diameter	N/A
	Average laser pulse density per m2	1200
	N/E/H accuracy (precision) (m)	N/A
	Number of flight strips	9
	Estimated type archaeology	ditches
	Estimated depth archaeology	10-100cm
	Vegetation type	Grassland
	Vegetation state	Recently moan
	Moisture conditions	Intermitted very light rain
	Superficial layer	Loam on Sand
	Soil matrix	Recently moan
	Light conditions	Intermitted very light rain
	Number of points	Ca. 122.000.000
	Format	.txt
<b>Geometric correction</b>	Flight trajectory calculation (software/method)	DJI Pilot/grid/DGPS
	GCPs used	N/A
	GNSS geolocation instrument	D-RTK 2 Mobile Station

	GNSS geolocation accuracy	1-2cm
	Raw data analysis	DJI Terra
	Merging of raw data with flight trajectory	DJI Terra
	GNSS and IMU merging	DJI Terra
	Full-Waveform Processing and Filtering	N/A
	LAS export	DJI Terra
	LAS format	1.4
	Coordinate system	Amersfoort/RD New (EGM 96 Geoid), EPSG: 28992
<b>Radiometric correction</b>	Processing and calibration	N/A
	Setting	N/A

## Appendix 2: data processing parameters

### Multispectral survey

<b>PG: Import/reference</b>	Software	Pix4D Mapper 4.5.7
	Batch/Chunks	5 (R/G/B/RE/NIR)
	Geolocated images	2990
	Quality check	Manual
	CRS camera	WGS84 (EGM 96 Geoid), EPSG: 4326
	CRS GCPs	N/A
	CRS output	WGS84 (EGM 96 Geoid), EPSG: 4326
	Camera model	RedEdge-M_5.5_1_1280x960 (R/G/B/RE/ NIR)
	Geolocation accuracy	Horz: 5m Vert: 5m
	Manual corrections	Set altitude to 80m
	Mean Reprojection Error	0.254 pixels
	GCPs used	N/A
	GCP accuracy	N/A
<b>PG: Alignment/sparse PC</b>	Keypoint Image Scale	Full
	Calibrated/aligned images	2980
	Matching type	Aerial Grid or Corridor
	Matching settings	None
	Key point extraction	Automatic (median of 10.000 per image)
	Tie point extraction	N/A
	Calibration method	Alternative
	Int. parameters optim.	All
	Ext. parameters optim.	All
	Rematch	Auto
	Other settings	N/A
<b>PG: Dense PC</b>	Image scale/quality	Multiscale, ½ (half image size, default)
	Point density	optimal
	Minimum # of matches	3
	Number of points	4136963

	Classification	No
	Other settings	N/A
<b>PG: 3D model</b>	Source data	N/A
	Surface type	N/A
	Octree depth	N/A
	Face count	N/A
	Texture size	N/A
	Texture source data	N/A
	Texture type	N/A
	Mapping mode	N/A
	Blending mode	N/A
	Colour balancing	N/A
	Other settings	N/A
<b>PG: ortho</b>	GSD	N/A
	Source data	N/A
	Blending mode	N/A
	Other settings	N/A
<b>PG: DSM</b>	GSD	N/A
	Source data	N/A
	Noise filter	N/A
	Surface smoothing	N/A
	Type	N/A
	Method	N/A
<b>PG: DTM</b>	GSD	N/A
	Point classes	N/A
<b>PG: index</b>	GSD	5.62cm/pixel
	Radiom. correction type	Camera and Sun Irradiance using DLS IMU
	Calibration	Yes (with reflectance target)
	Reflectance map	Yes
	Index and calculation	R, G, B, RE, NIR $NDVI = (NIR-R)/(NIR+R)$

		ARVI = $(nir - (2 * red) + blue) / (nir + (2 * red) + blue)$ NDWI = $(green - nir) / (green + nir)$ NDRE = $(nir - red\_edge) / (nir + red\_edge)$
<b>Enhanced visualisation</b>	Software	QGIS 3.32.2
	Visualisation	Singleband pseudocolour
	Colour ramp	RdGy
	Processing	None
	Filter	Local cumulative cut stretch (set by window extents, default settings)
	Settings	None

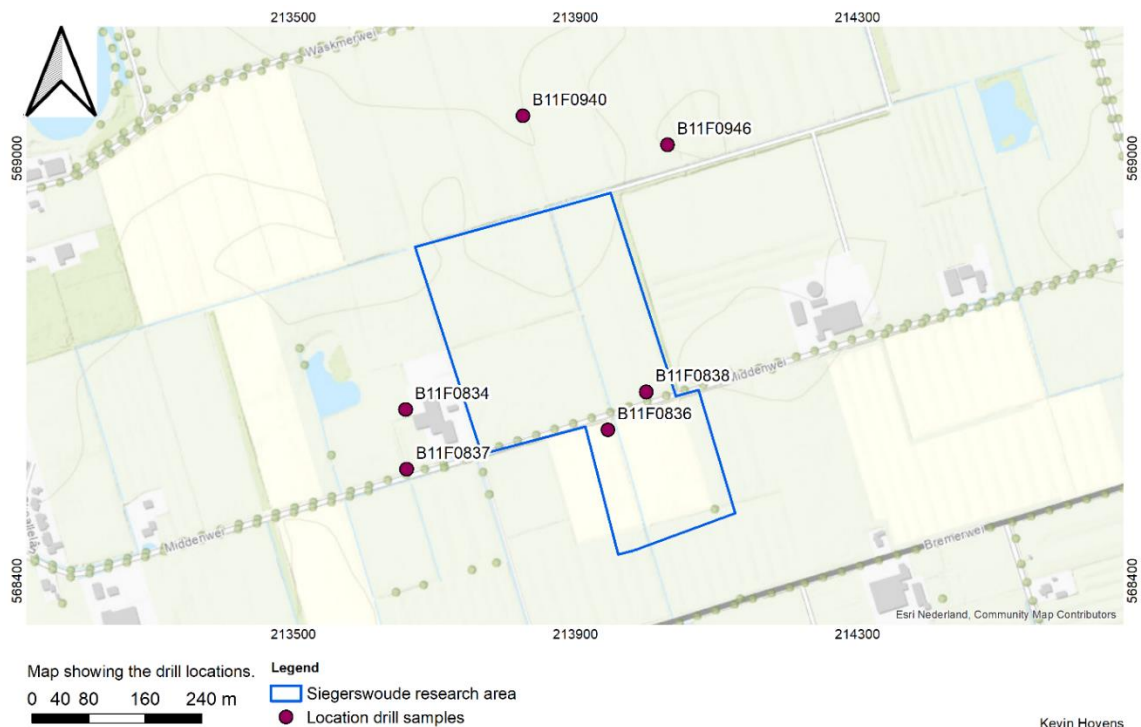
## LiDAR survey

<b>Conversion</b>	Software	LAStools Rapidlasso GmbH
	Tool	Tiling
	Filter	None
	Settings	20m
	Script	<code>lastile -i *.las -tile_size 20 -buffer 2 -odir 1-tiles -o tile.laz</code>
<b>Automatic ground point classification</b>	Software	LAStools Rapidlasso GmbH
	Tool	Ground point
	Filter	Ground point
	Settings	Extra fine, Wilderness
	Script	<code>lasground -i *.laz -odir 2-ground -o ground.laz -extra_fine -wilderness</code>
<b>DTM</b>	Software	LAStools Rapidlasso GmbH
	Tool	DEM
	Filter	None
	Settings	Resolution 0.005m, ignore triangles of >50m
	Script	<code>las2dem -i *.laz -odir 3-dem -o dem.tif -use_tile_bb -keep_class 2 -step 0.005 -kill 50</code>
<b>Merge</b>	Software	QGIS 3.32.2
	Tool	Merge
	Filter	None
	Settings	None

	Script	None
<b>Enhanced visualisation</b>	Software	QGIS 3.32.2
	Visualisation	Multiband colour
	Red band	Min: 45,1851 Max: 46,7837
	Green band	Min: - Max: -
	Blue band	Min: - Max: -
	Processing	None
	Filter	Local cumulative cut stretch (set by window extents, default settings)
	Settings	None

## Appendix 3: coring samples

The images of the soil cores and their locations were obtained from DINOloket (TNO Geologische Dienst Nederland, 2023).



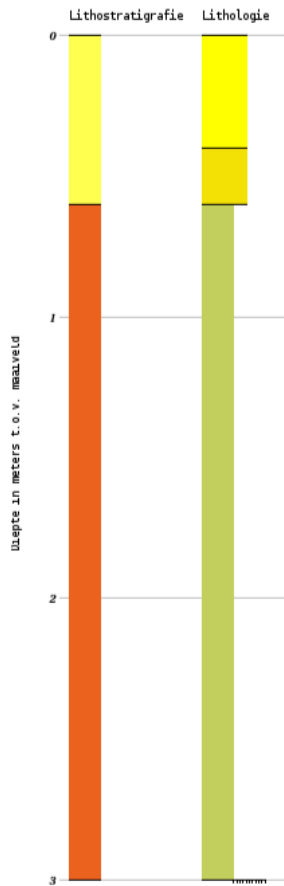
Figuur 1: Research area with the coring locations (TNO Geologische Dienst Nederland, 2023; own work)

On the following pictures, the lithology is in Dutch. Therefore, a translation is provided:

Leem:	loam
Zand fijn categorie:	sand fine grain category
Zand midden categorie:	sand medium grain category
Veen:	Peat

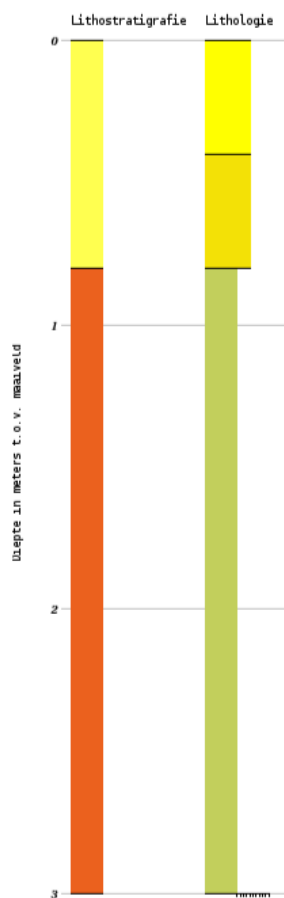
On the images, abbreviations of lithostratigraphic designations are also included. The complete designations are provided:

AAOP:	“antropogeen, opgebrachte grond” (brought-in soil)
NIGR:	“Formatie van Nieukoop, Laagpakket van Griendstveen”
BXWI:	“Formatie van Boxtel, Laagpakket van Wierden”
DRGI:	“Formatie van Drente, Laagpakket van Gieten”
DN:	“Formatie van Drachten”



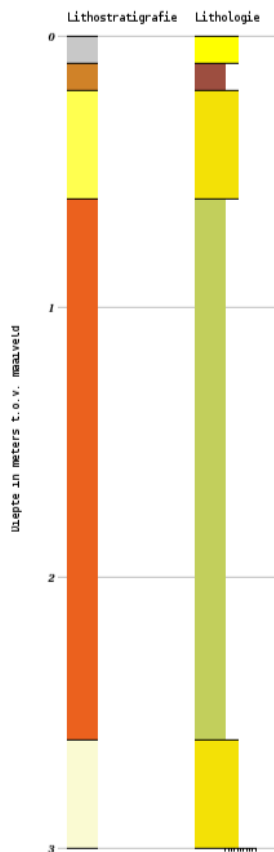
Identification : B11F0834  
 Coordinates : 213660 , 568640 (RD)  
 Ground level: 5.00 m t.o.v. NAP  
 Available information: Digital recording data  
 Description method: Unknown  
 Quality interpretation: Not validated in subsurface model

<b>Lithostratigrafie</b>	<b>Lithologie</b>
BXWI	Leem
DRGI	Zand fijne categorie
	Zand midden categorie

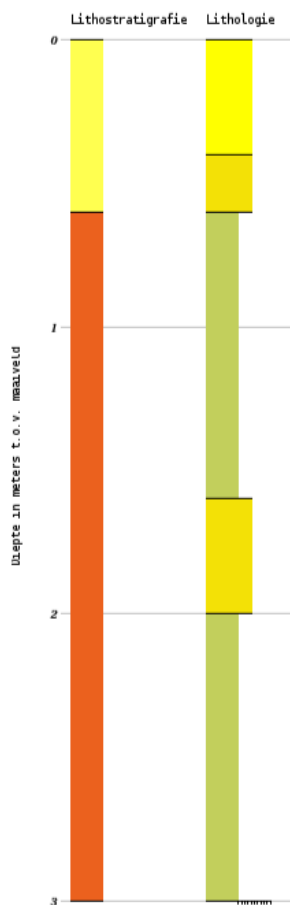


Identification : B11F0836  
 Coordinates : 213950 , 568620 (RD)  
 Ground level: 4.70 m t.o.v. NAP  
 Available information: Digital recording data  
 Description method: Unknown  
 Quality interpretation: Not validated in subsurface model

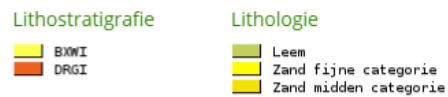
<b>Lithostratigrafie</b>	<b>Lithologie</b>
BXWI	Leem
DRGI	Zand fijne categorie
	Zand midden categorie

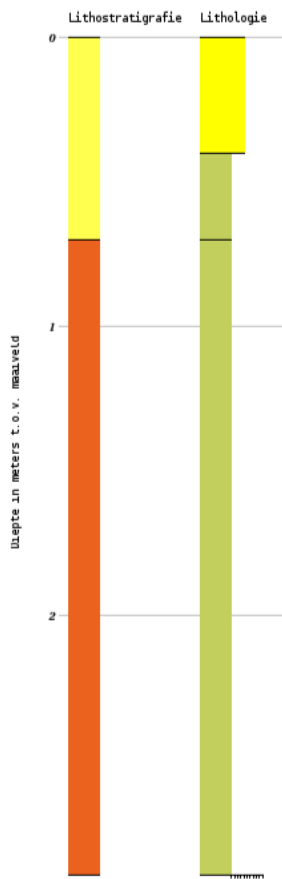


Identification : B11F0837  
 Coordinates : 213660 , 568560 (RD)  
 Ground level: 4.60 m t.o.v. NAP  
 Available information: Digital recording data  
 Description method: Unknown  
 Quality interpretation: Not validated in subsurface model



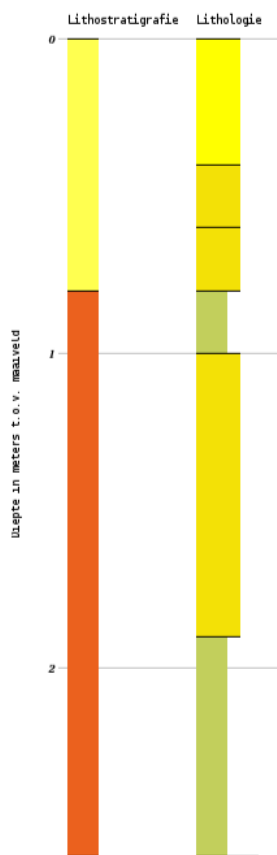
Identification : B11F0838  
 Coordinates : 214000 , 568670 (RD)  
 Ground level: 4.80 m t.o.v. NAP  
 Available information: Digital recording data  
 Description method: Unknown  
 Quality interpretation: Validated in subsurface model





Identification : B11F0940  
 Coordinates : 213690 , 569000 (RD)  
 Ground level: 5.30 m t.o.v. NAP  
 Available information: Digital recording data  
 Description method: Unknown  
 Quality interpretation: Not validated in subsurface model

**Lithostratigrafie**      **Lithologie**  
 B/WI       Leem  
 DRGI       Zand fijne categorie



Identification : B11F0946  
 Coordinates : 214000 , 569000 (RD)  
 Ground level: 5.00 m t.o.v. NAP  
 Available information: Digital recording data  
 Description method: Unknown  
 Quality interpretation: Not validated in subsurface model

**Lithostratigrafie**      **Lithologie**  
 B/WI       Leem  
 DRGI       Zand fijne categorie  
 Zand midden categorie